

General Disclaimer

One or more of the Following Statements may affect this Document

- This document has been reproduced from the best copy furnished by the organizational source. It is being released in the interest of making available as much information as possible.
- This document may contain data, which exceeds the sheet parameters. It was furnished in this condition by the organizational source and is the best copy available.
- This document may contain tone-on-tone or color graphs, charts and/or pictures, which have been reproduced in black and white.
- This document is paginated as submitted by the original source.
- Portions of this document are not fully legible due to the historical nature of some of the material. However, it is the best reproduction available from the original submission.

NASA TECHNICAL
MEMORANDUM

NASA TM X-53772

August 23, 1968

NASA TM X-53772

GPO PRICE \$ _____

CFSTI PRICE(S) \$ _____

Hard copy (HC) 3.00

Microfiche (MF) .65

ff 653 July 65

THE NONDESTRUCTIVE EVALUATION OF STRESS-CORROSION
INDUCED PROPERTY CHANGES IN ALUMINUM

By W. N. Clotfelter, B. F. Bankston and
E. E. Zachary
Propulsion and Vehicle Engineering Laboratory

NASA

N 68-35652
(ACCESSION NUMBER)
44
(PAGES)
TMX-53772
(NASA CR OR TMX OR AD NUMBER)

(THRU)
1
(CODE)
17
(CATEGORY)

George C. Marshall
Space Flight Center,
Huntsville, Alabama



TECHNICAL MEMORANDUM X-53772

THE NONDESTRUCTIVE EVALUATION OF STRESS-CORROSION
INDUCED PROPERTY CHANGES IN ALUMINUM

by

W. N. Clotfelter, B. F. Bankston, and E. E. Zachary

George C. Marshall Space Flight Center

Huntsville, Alabama

ABSTRACT

The problem of stress corrosion failures has plagued most current aerospace vehicles. In an attempt to establish a better understanding of this phenomenon and to develop methods by which it might be depicted in early stages, experiments were designed to investigate methods by which potential stress corrosion failures could be evaluated during the period of incubation. These experiments involved very precise measurements of selected physical property changes in the material during the onset of stress corrosion. Both highly susceptible and highly resistant materials were included in the experimental program. The resultant data show clearly that the period of stress corrosion incubation can be detected nondestructively in the highly susceptible alloys.

NASA-GEORGE C. MARSHALL SPACE FLIGHT CENTER

NASA - GEORGE C. MARSHALL SPACE FLIGHT CENTER

TECHNICAL MEMORANDUM X- 53772

THE NONDESTRUCTIVE EVALUATION OF STRESS-CORROSION
INDUCED PROPERTY CHANGES IN ALUMINUM

by

W. N. Clotfelter, B. F. Bankston, and E. E. Zachary

PROPELLION & VEHICLE ENGINEERING LABORATORY
RESEARCH AND DEVELOPMENT OPERATIONS

ACKNOWLEDGEMENT

The authors are indebted to J. G. Williamson, T. S. Humphries, and E. E. Nelson of the Metallic Materials Branch for assistance in planning this program and for laboratory assistance in stressing and corroding the required specimens.

TABLE OF CONTENTS

	Page
SUMMARY.....	1
INTRODUCTION.....	1
ELECTRICAL CONDUCTIVITY MEASUREMENTS.....	3
ULTRASONIC SURFACE WAVE ATTENUATION MEASUREMENTS.....	5
INTERNAL FRICTION MEASUREMENTS.....	8
CONCLUSIONS	10

LIST OF ILLUSTRATIONS

Figure	Title	Page
1.	BLOCK DIAGRAM OF A TYPICAL EDDY CURRENT SYSTEM.....	12
2.	A HIGH FREQUENCY EDDY CURRENT INSTRUMENT.....	13
3.	A LOW FREQUENCY EDDY CURRENT INSTRUMENT.....	14
4.	FLAT SPECIMEN STRESSING TECHNIQUE.....	15
5.	CONDUCTIVITY, STRESS AND FREQUENCY RELATIONSHIPS IN 7079-T6 ALUMINUM.....	16
6.	DEGRADATION OF 7079-T6 ALUMINUM BY STRESS CORROSION....	17
7.	ELECTRICAL CONDUCTIVITY VS. TIME FOR CORRODED 2219-T31 ALUMINUM.....	18
8.	ELECTRICAL CONDUCTIVITY VS. TIME FOR CORRODED 2219-T31 ALUMINUM.....	19
9.	ELECTRICAL CONDUCTIVITY VS. TIME FOR CORRODED 2219-T81 ALUMINUM.....	20
10.	ELECTRICAL CONDUCTIVITY VS. TIME FOR CORRODED 2219-T81 ALUMINUM.....	21
11.	SNELL'S LAW.....	22

LIST OF ILLUSTRATIONS (Concluded)

Figure	Title	Page
12.	BLOCK DIAGRAM OF A TYPICAL ULTRASONIC SYSTEM.....	23
13.	ULTRASONIC SURFACE WAVE TECHNIQUE.....	24
14.	ULTRASONIC SURFACE WAVE ATTENUATION OF DEGRADED 7079-T6 ALUMINUM.....	25
15.	ATTENUATION OF 5 MHZ ULTRASONIC SURFACE WAVES IN CORRODED 7079-T6 ALUMINUM.....	26
16.	ATTENUATION OF 5 MHZ ULTRASONIC SURFACE WAVES IN CORRODED 2219-T31 ALUMINUM.....	27
17.	ATTENUATION OF 5 MHZ ULTRASONIC SURFACE WAVES IN CORRODED 2219-T31 ALUMINUM.....	28
18.	ATTENUATION OF 5 MHZ ULTRASONIC SURFACE WAVES IN CORRODED 2219-T81 ALUMINUM.....	29
19.	ATTENUATION OF 5 MHZ ULTRASONIC SURFACE WAVES IN CORRODED 2219-T81 ALUMINUM.....	30
20.	ELASTOMAT AND VACUUM CHAMBER.....	31
21.	STRESSING FIXTURE FOR CYLINDRICAL SPECIMEN.....	32
22.	SPECIMEN SUPPORT FOR INTERNAL FRICTION MEASUREMENTS..	33
23.	INTERNAL FRICTION OF 7079-T6 ALUMINUM VIBRATING IN THE TRANSVERSE MODE.....	34
24.	INTERNAL FRICTION OF CORRODED 7079-T6 ALUMINUM VIBRATING IN THE TORSIONAL MODE.....	35
25.	INTERNAL FRICTION OF CORRODED 7079-T6 ALUMINUM VIBRATING IN THE TORSIONAL MODE.....	36

TECHNICAL MEMORANDUM X-53772

THE NONDESTRUCTIVE EVALUATION OF STRESS-CORROSION INDUCED PROPERTY CHANGES IN ALUMINUM

SUMMARY

The development of high strength aluminum alloys for use in the aerospace industry has improved strength to weight ratios significantly. Many of these alloys, however, are highly susceptible to stress corrosion cracking. The fundamental mechanisms of stress corrosion on a microscopic basis are not well understood and no method is available today for determining stress corrosion "damage" prior to failure.

A program was initiated to develop a better understanding of stress corrosion mechanisms, to determine rapid, practical means of evaluating stress-corrosion susceptibility, and to measure stress corrosion related material property changes nondestructively. Measurements of dynamic modulus, internal friction, electrical conductivity, and ultrasonic surface wave attenuation have been made on aluminum alloys 7079-T6, 2219-T31, and 2219-T81 as a function of the onset of stress corrosion. All measurements were successful in depicting stress corrosion in 7079-T6 and 2219-T31. Although similar indications were measured in 2219-T81, the same indications were shown when this alloy was exposed only to corrosion degradation. This result is significant in that the 2219-T81 alloy is resistant to stress corrosion and therefore, the impact of stress corrosion degradation was shown to be no greater than that of atmospheric corrosion.

INTRODUCTION

Material problems created by stress corrosion cracking are numerous and well known. Some premature failures of components for Saturn vehicles have been caused by stress corrosion. Specifically, several liquid oxygen domes made of 7079-T6 aluminum have cracked. Small MC sleeves of AM 355 stainless steel used on tubing have also failed by stress corrosion cracking. Springs of 17-7 PH steel have failed due to the same reason. Stress corrosion is also a major problem of military and commercial aircraft reliability in that many failures have been attributed to this cause.

Stress corrosion cracking is characterized by localized, brittle-type fractures in otherwise ductile material [1]. The cracks

propagate perpendicularly to the stress load direction on the surface. Initial stress corrosion cracking in aluminum is intergranular although both intergranular and transgranular cracking occurs in the later stages of the process. The relative susceptibilities of various aluminum alloys and the effects of temper and surface treatments have been established for most engineering alloys. The threshold stress required to initiate stress corrosion in aluminum has been determined to be at seven or eight thousand pounds per square inch for some of the more susceptible alloys when stressed in the short transverse grain direction. Short transverse is perpendicular to the rolling direction through the smaller dimension of the material. However, the fundamental causes of material degradation by stress corrosion on a microscopic basis are not well understood. Some observers say a high density of dislocation loops make an alloy susceptible to stress corrosion. Macroscopic parameters affecting the occurrence and the rate of stress corrosion cracking are time, temperature, corrosive environment, chemistry of the alloy, residual or applied tensile stress, and grain orientation with respect to stress.

Little can be done about the time that susceptible alloys are exposed to corrosive environments. Strength requirements determine the particular alloy to be used. The magnitude of residual stresses is difficult to control and to measure. Careful design can in some applications prevent high tensile stress from being applied in the short transverse direction. Aluminum alloys exposed in the short transverse direction are most susceptible to stress corrosion cracking. Thus, until improved alloys are available, one approach to this corrosion problem is to evaluate residual stress and stress corrosion damage non-destructively. In this way, probable component failures can be identified and replaced before failure. Nondestructive means of measuring residual stress are being developed and will be described in other reports. Reliable techniques of evaluating stress corrosion damage nondestructively are not now available. However, a shortage of testing methods is not the major difficulty. A wide range of instrumentation is available for measuring most material properties nondestructively. The problem consists of identifying early stages of the material condition that will result in component failure. When this problem is solved, the development of practical NDT methods for measuring stress corrosion damage will not be difficult. Thus, the ultimate objectives of this program are the development of practical nondestructive techniques for measuring stress corrosion susceptibility and stress corrosion damage. The immediate goal is the measurement of stress corrosion damage or material property changes in the laboratory as an aid in understanding stress corrosion mechanisms.

Initially, several nondestructive methods were considered feasible for evaluating material property changes near the surface of metals. These methods were electrical conductivity, attenuation of ultrasonic

surface waves, internal friction measurements, dynamic modulus, and acoustic emission. Dynamic modulus was eliminated as a candidate technique by initial experiments. The value of acoustic emission measurements is questionable. The other three techniques listed above will be discussed in this report.

ELECTRICAL CONDUCTIVITY MEASUREMENTS

The electrical conductivity of metals is a very sensitive and easily measured property which can be used to learn much about the condition of metallic materials. Conductivity measurements have been used to investigate phase transformations, age hardening, order-disorder changes and constitutional diagrams [2]. A perfect lattice offers very little resistance to the passage of electrons. Many factors increase this basic resistance. These include lattice defects such as vacancies, dislocations, interstitial ions, and stacking faults. Alloying, impurity atoms, grain boundaries, plastic and elastic deformation also affect resistance. These factors affect resistance to varying degrees. Alloying, grain boundaries and impurity atoms have rather large effects on resistance. The effect of elastic deformation is small. Tensile strain increases resistance. In most metals there is a decrease in resistance with pressure. Dislocations contribute to resistivity in certain directions, but have no effect in the direction of the dislocation axis. Severe corrosion has a large effect on the surface conductivity of metals. Furthermore, the wide range of defects and conditions which affect electrical conductivity suggests that defects caused by the early stages of stress corrosion can also be detected by conductivity measurements.

The early stage of stress corrosion cracking is a surface phenomenon. Evaluation techniques must be capable of measuring only surface and near surface property changes to be effective. Electromagnetic techniques such as eddy current and microwave are ideally suited for the purpose, since the depth of measurement may be controlled by selecting various operational inspection frequencies. Thus penetration of induced high frequency currents may be calculated as indicated below [3].

$$\alpha = 5.03 \sqrt{\frac{\rho}{\mu f}} \text{ centimeters}$$

where:

α = depth of current penetration

ρ = resistivity in micro ohm centimeters

μ = relative permeability

f = frequency in hertz

5.03 = a constant based on units.

Eddy current instruments consist of a variation of the basic wheatstone bridge, an oscillator, an amplifier, a null indicator, and a calibrated readout. A block diagram is shown in Figure 1. A transducer or coil which forms one leg of the bridge circuit is the measuring probe. The specimen electrical conductivity determines the magnitude of induced current which is reflected into the transducer as an impedance change that unbalances the bridge. A calibrated dial or scale indicates the magnitude of the bridge unbalance which is a measure of conductivity. Subsequent to an initial balancing of the bridge and to sensitivity adjustments with the transducer on materials of known conductivity, the instrument is ready for use.

A range of frequencies is necessary to study corrosion damage as a function of depth in metals. The Dermitron Thickness Tester* is a specialized type of eddy current instrument that operates at 100, 500, 2,000 and 6,000 kilohertz. Electrical conductivity measurements can be made on 1/8 inch diameter spots. The Dermitron is shown in Figure 2.

A magnatest conductivity meter type FM-120** was also used. This instrument operates at 60 kilohertz and uses a 1/2 inch diameter transducer. The FM-120 instrument is shown in Figure 3.

Materials being investigated are 7079-T6, 2219-T3, and 2219-T81 aluminum. Specimens are two and one-half by six by three sixteenths inches in size. Materials have been exposed in the short transverse and in the longitudinal directions. The specimens are clamped in a bent position which loads the center portion at the surface to 75 percent of the yield strength. This is illustrated in Figure 4. The corrosive environment consists of a ten-minute exposure every hour to a three and one-half percent salt solution. Deionized water is used to make the solution. Specimens were removed from the alternate immersion tester at regular intervals for evaluation. Subsequent to removal the applied stress was released, the specimens were cleaned with a 20 percent HNO_3 + 5 percent HF solution, rinsed with H_2O , and passivated with 70 percent HNO_3 solution.

Figure 5 depicts conductivity changes along the length of an aluminum specimen which had previously been subjected to an environment which induces stress corrosion. This specimen had been clamped in a bent position with maximum stress at the center portions as shown in Figure 4. Applied stress was removed before conductivity measurements were made. Changes in surface conditions caused by stress corrosion of specimens cut in the short transverse direction are clearly shown in the curves of Figure 5. This figure also illustrates how the frequency of

* Product of Unit Process Assemblies, Incorporated

** Product of Magnaflux Corporation

electromagnetic energy affects the depth of current penetration and thus the apparent conductivity of surface layers in metals. Obviously, higher frequencies are more sensitive to near-surface property changes. Thus, even higher frequencies may be used to detect the initial stages of stress corrosion damage.

Stress corrosion induced material degradation as a function of time is depicted in Figure 6. A frequency of six megahertz was used to obtain this curve. Data for the curves discussed in the preceding paragraph were obtained from aluminum surfaces which were in tension during the stress corrosion process. There was no significant change in the conductivity of the compressed side of the specimen. Furthermore, neither tensile stress alone nor the very early stages of corrosion alone has much effect on electrical conductivity. This is true for specimens cut in the short transverse and the longitudinal (rolling) direction. Thus, high frequency measurements of electrical conductivity are an effective way to detect early stages of stress corrosion damage in 7079-T6 aluminum.

Machine finished and chemically milled specimens of 2219-T31 and 2219-T81 alloys were corroded and subsequently evaluated nondestructively. Results are shown in Figures 7 through 10. The objective in chemically milling some of the material was to remove surface residual stresses and possibly reduce spread in the data. However, the only apparent effect was to reverse the conductivity relationship between the stress corroded material and material subjected to corrosion only. That is, smaller conductivity changes occurred in stress corroded specimens than in those subjected to corrosion only. As shown in Figure 7, the electrical conductivity method of detecting stress corrosion damage in machine finished 2219-T31 aluminum is effective. This is not true for 2219 aluminum in the T81 condition as illustrated in Figure 9.

Stress corrosion degrades the surface of susceptible metals rapidly. This material damage results in electrical conductivity changes which are related to the degree of degradation. The precise cause of conductivity changes during the early stages of stress corrosion is not entirely understood. This aspect of the corrosion problem is being investigated with metallographic techniques. Future work will include correlation of destructive and nondestructive tests and the development of more practical high frequency eddy current systems.

ULTRASONIC SURFACE WAVE ATTENUATION MEASUREMENTS

Ultrasonic stress wave propagation is affected by many variables. The effects of all these parameters can be evaluated by making velocity and attenuation measurements of these stress waves. Surface wave

velocities are determined by the modulus of rigidity and the material density, but stress corrosion has little effect on modulus or density. Ultrasonic attenuation is much more sensitive to minute defects in metals and will be discussed in greater detail.

Strain, frequency, grain orientation, and temperature affect the attenuation of ultrasonic waves. Loss mechanisms include scattering by point defects and grain boundaries, absorption by dislocation and thermoelastic damping. Transducer coupling and gross defects cause additional losses. Thus, ultrasonic technology has furnished a very sensitive tool for investigating the properties of materials.

Ultrasonic techniques have been used to measure modulus, grain size, radiation damage and to evaluate the effectiveness of various heat treatments of metals [4]. Ultrasonic methods have also been used to study internal oxidation in alloys, the effects of hydrogen in metals, and the properties at cryogenic temperatures. In short, almost anything that degrades or modifies metals can be detected ultrasonically.

As previously stated, the early stage of stress corrosion cracking is a surface phenomenon. Evaluation techniques must be capable of measuring only surface and near surface property changes to be effective. Like the eddy current method, ultrasonic surface waves can be used to evaluate surface layers of a specified depth. In this case the depth of penetration is approximately equal to one wavelength of sound in the material being investigated. Since wavelength is equal to velocity divided by frequency, high frequencies can be used to investigate very thin layers of material.

Surface waves can be generated with Y-cut quartz transducer crystals mounted parallel to the surface or with X-cut crystals mounted on a lucite wedge at an angle. Crystals cut in the "Y" direction vibrate in a transverse direction making the generation of surface waves easy. X-cut crystals vibrate in the longitudinal direction and require an intermediate material, such as lucite, to transform them into surface waves. This can be explained in the following manner. When ultrasonic surface waves are propagated from one material to another at an angle, transformations occur at the boundary. This angular transmission is controlled by Snell's law which states:

$$\frac{\sin \phi_1}{V_1} = \frac{\sin \phi_2}{V_2}$$

Where ϕ_1 = angle of incident wave from the normal in first medium

ϕ_2 = angle of refracted wave from normal in second medium

v_1 = velocity of sound in first medium

v_2 = velocity of sound in second medium

When ϕ_1 is adjusted to make ϕ_2 equal 90° surface waves will be generated [11]. The exact angle of the wedge is selected to meet requirements of the formula.

A pulsed ultrasonic system was used to measure surface wave attenuation in aluminum. Systems of this type consist of a power supply, a pulser, timing circuits, amplifiers and a cathode ray tube display system. A signal controlled by the basic timing circuit triggers the oscillator which produces a pulse of radio-frequency energy of only a few microseconds duration. This electrical pulse is converted to mechanical energy with a piezoelectric transducer. The pulse repetition rate is adjusted to allow time for each pulse to be reflected from the specimen before additional pulses are triggered. Reflected pulses are amplified and displayed on the cathode ray tube. Distance from left to right on the base line of the oscilloscope represents increasing time; or the location of a pulse represents the distance of a reflecting surface from the transducer. A block diagram of a typical system is shown in Figure 12.

The same specimens were used for electrical conductivity and ultrasonic attenuation measurements. However, for the ultrasonic measurements, one end of each specimen was machined to eliminate the hole near the end which was used in the stressing process. The machined end served as a uniform reflecting surface for the ultrasonic energy as illustrated in Figure 13. All measurements are compared to results obtained from uncorroded specimen. No attempt has been made to make absolute attenuation measurements.

Ultrasonic surface waves are very sensitive to what appears to be stress corrosion damage. This is well illustrated in Figure 14, A through G and Figure 15. The pulse located at point "1" represents the transducer-metal interface. The magnitude of the back reflection at point "2" is a measure of energy losses near the surface. Rapid attenuation of the back reflection with time of exposure shows potential for the technique as a means of evaluating stress corrosion damage in 7079-T6 aluminum. Furthermore, tensile stresses, in the elastic range, alone have little or no residual effect on the attenuation of ultrasonic surface waves. A specimen was stressed to 75 percent of yield strength for 506 hours in air. Attenuation measurements were made subsequent to load removal with no apparent loss of energy. Figure 14-H illustrates

this fact.

Machine finished and chemically milled specimens of 2219-T31 and 2219-T81 aluminum were corroded and subsequently measured with ultrasonic surface wave attenuation techniques. Results are presented in Figures 16 through 19. Obviously, both corrosion and stress corrosion "damage" attenuate ultrasonic surface waves very rapidly in these alloys. In fact, the attenuation is so great in both cases, that this technique is not effective for the nondestructive evaluation of the early stages of stress corrosion damage in 2219 aluminum.

Although the ultrasonic surface wave technique is promising for susceptible alloys more work must be accomplished before firm conclusions are drawn concerning the practicality of using the method to measure stress corrosion damage in the field. Future work will involve transducer development and correlation studies of destructive and non-destructive results. The objective of correlation studies is obvious. Transducer development work will be directed toward the reduction of coupling problems.

INTERNAL FRICTION MEASUREMENTS

The amplitude of any vibrating body will decay when the driving force is removed. The rate of decay is less in a vacuum than in air; but, the vibrational energy is still dissipated. Numerous mechanisms causing this internal loss of energy determine the "damping capacity" or "internal friction" of the material. Many factors affect the internal friction of metals. These include, but are not limited to the ordering of solute atoms, movement of dislocations in single crystals, slip along grain boundaries, thermoelastic effects and scattering by grains.

Damping capacity measurements can be used to study the internal structure and atomic movements in solids^{2, 6, 7, and 8}. This method has also been used to study the effects of radiation, heat treatment and corrosion on metals. In short, an abundance of literature is available describing the sensitivity of the method to point, line and other minute defects in metals. Although the exact mechanisms causing this internal loss of energy are difficult to identify and to measure, the technique appears feasible as a means of measuring stress corrosion damage in the laboratory. More information can be obtained by making damping measurements at different temperatures and frequencies. However, the immediate objective of this phase of the program is simply to determine whether or not changes in internal friction values can be used to detect stress corrosion damage.

Several ways of measuring internal friction are described in Reference 6. These methods are:

1. Measurement of the energy input required to maintain a specimen in vibration at constant amplitude.
2. Measurement of some response of a system, e.g., the displacement of the end of a rod specimen, when in forced oscillation under a periodic force whose frequency is varied.
3. Measurement of decay of free vibrations of a specimen.
4. Measurement of the attenuation of a progressive wave through the material.

The decay rate of free vibrations was used to obtain results given in this report. The instrumentation is shown in Figure 20. A vacuum chamber has been added to the commercial instrument to reduce air damping losses from vibrating specimens. This is necessary since the energy loss to the air from a vibrating specimen can be as high as the change in internal friction caused by stress corrosion.

A standard cylindrical tensile specimen configuration was selected to provide for uniform stressing and the required damping measurements. The stressing fixture is shown in Figure 21. Subsequent to being exposed to an environment which induces stress corrosion, the threaded ends were removed from the specimens leaving a uniform cylinder 3/16 inch in diameter and 2.6 inches long. This small diameter was chosen so the surface area exposed to corrosion would be high compared to the cross sectional area. Specimens 1/8 inch in diameter were also used, but the results were not as repeatable.

Magnetic vibrating techniques are very effective for damping measurements since mechanical contact is not required between transducers and the specimen. Since this program involved non-magnetic aluminum specimens, small magnetic disks were attached to the ends of the specimen with strain gage cement. The specimen was supported on thin wires as pictured in Figure 22 and vibrated at its natural resonant frequency. Driving energy was then removed and the vibration decay rate was measured. Losses are expressed as a logarithmic decrement,

$$\delta = \log_e \left(\frac{A_n}{A_{n+1}} \right)$$

where A_n is the amplitude of decaying vibration and A_{n+1} is the amplitude of the successive vibration.

Typical results are plotted in Figure 23. As the curves indicate, the damping capacity of aluminum is very sensitive to stress corrosion damage.

The curves plotted in Figure 23 were obtained with specimens vibrating in the transverse mode. Other specimens of the same alloy were vibrated in the torsional mode. Comparative results shown in Figure 24 and Figure 25 were obtained from specimens vibrating in a vacuum (10 microns) and in air, respectively. The same shaped curves were obtained in both cases. Thus, the torsional technique of measuring internal friction is even more sensitive than the transverse mode.

Data for the curves were obtained using specimens machined in the short transverse direction. Specimens cut in the longitudinal direction followed the same general pattern, but the magnitude of the energy losses was much less. Early stages of corrosion alone had little effect on the damping capacity of specimens cut either way. The exact mechanisms causing increased energy losses in specimens subjected to stress corrosion have not been determined. This aspect of the problem will be investigated. Additional future work will include the investigation of other alloys, damping measurements as functions of frequency and temperature. Attempts will also be made to correlate the magnitude of damping losses with metallographic information.

CONCLUSIONS

The magnitude of electrical conductivity values, ultrasonic surface wave attenuation, and internal friction loss is changed by the stress corrosion of 7079-T6 aluminum. Stress corrosion also causes a rapid decrease in the electrical conductivity of 2219-T31 aluminum. Corrosion only, has much less effect on this alloy. Thus, a nondestructive testing potential exists for 7079-T6 and 2219-T31 aluminum alloys.

No significant difference was observed in the electrical conductivity of 2219-T81 specimens exposed to stress corrosion and those exposed to corrosion only. This is as expected since 2219-T81 material is not susceptible to stress corrosion cracking. Both stress corrosion and corrosion alone cause rapid attenuation of ultrasonic surface waves in 2219-T31 and 2219-T81 aluminum. No attempt will be made at this time to identify or to describe the exact mechanisms causing the observed results. Subsequent to planned metallurgical examinations of degraded materials more information will be reported.

Low frequency internal friction measurements appear to be useful only as a means of studying stress corrosion mechanisms in the laboratory. It is doubtful that this particular method could be adapted

to the practical evaluation of degraded materials in actual components.

Results of this program indicate that the eddy current or conductivity method is superior to the ultrasonic method of measuring stress corrosion damage in certain aluminum alloys. Coupling energy into the material is easier in the eddy current case. However, more work is required to determine the full potential and limitations of each method.

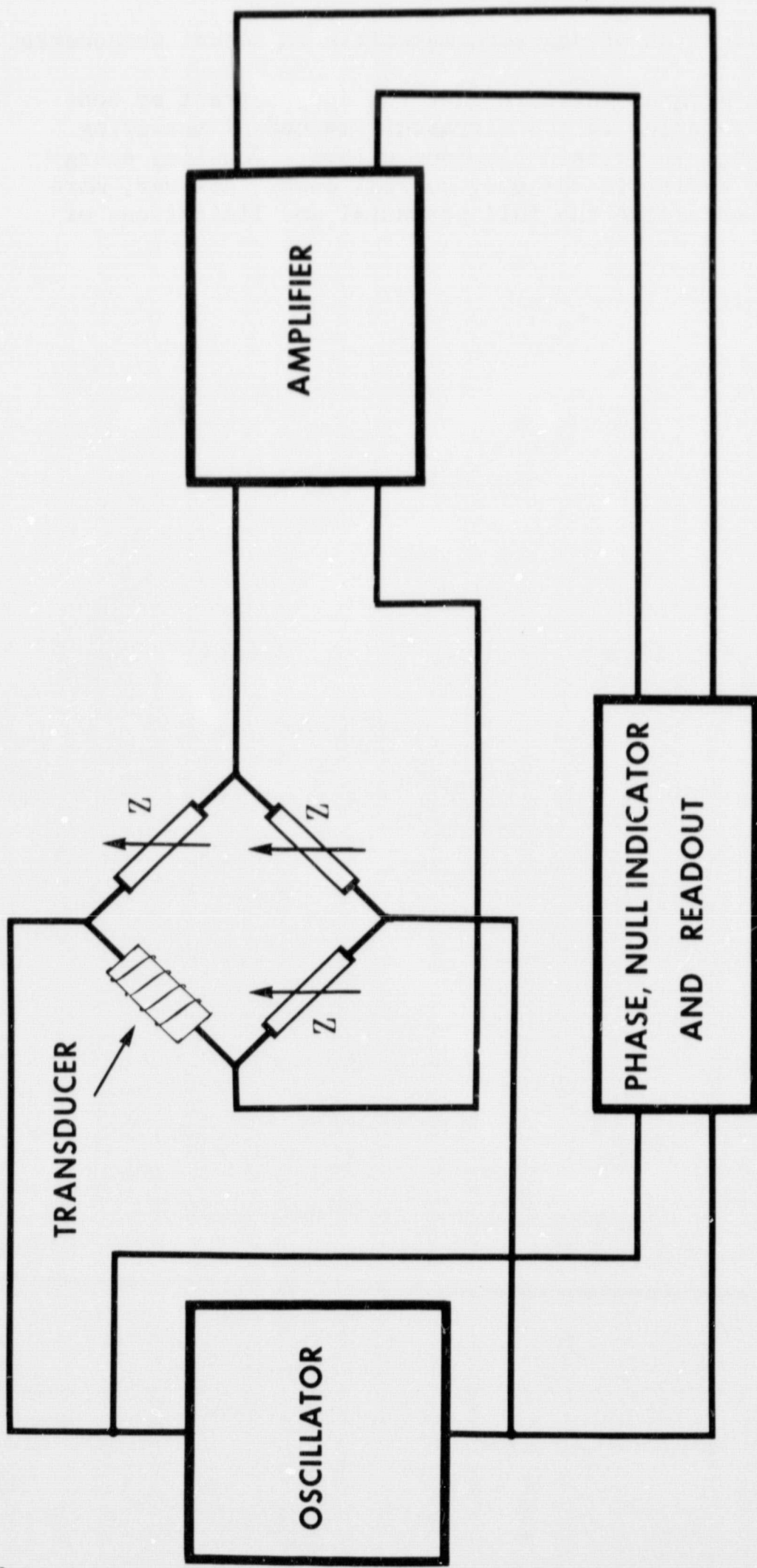


FIGURE 1: BLOCK DIAGRAM OF A TYPICAL EDDY CURRENT SYSTEM

FIGURE 2: A HIGH FREQUENCY EDDY CURRENT INSTRUMENT

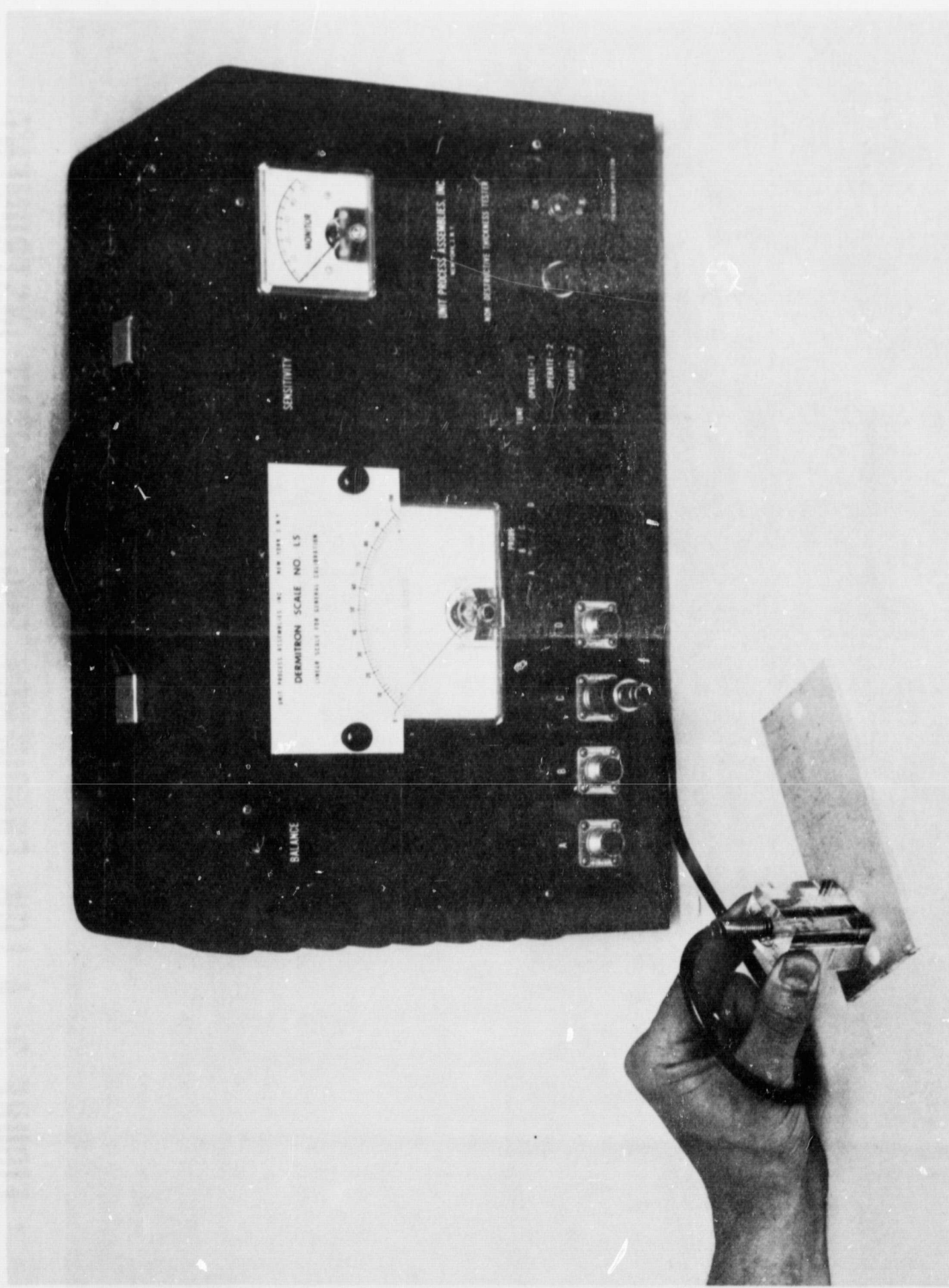


FIGURE 3: A LOW FREQUENCY EDDY CURRENT INSTRUMENT

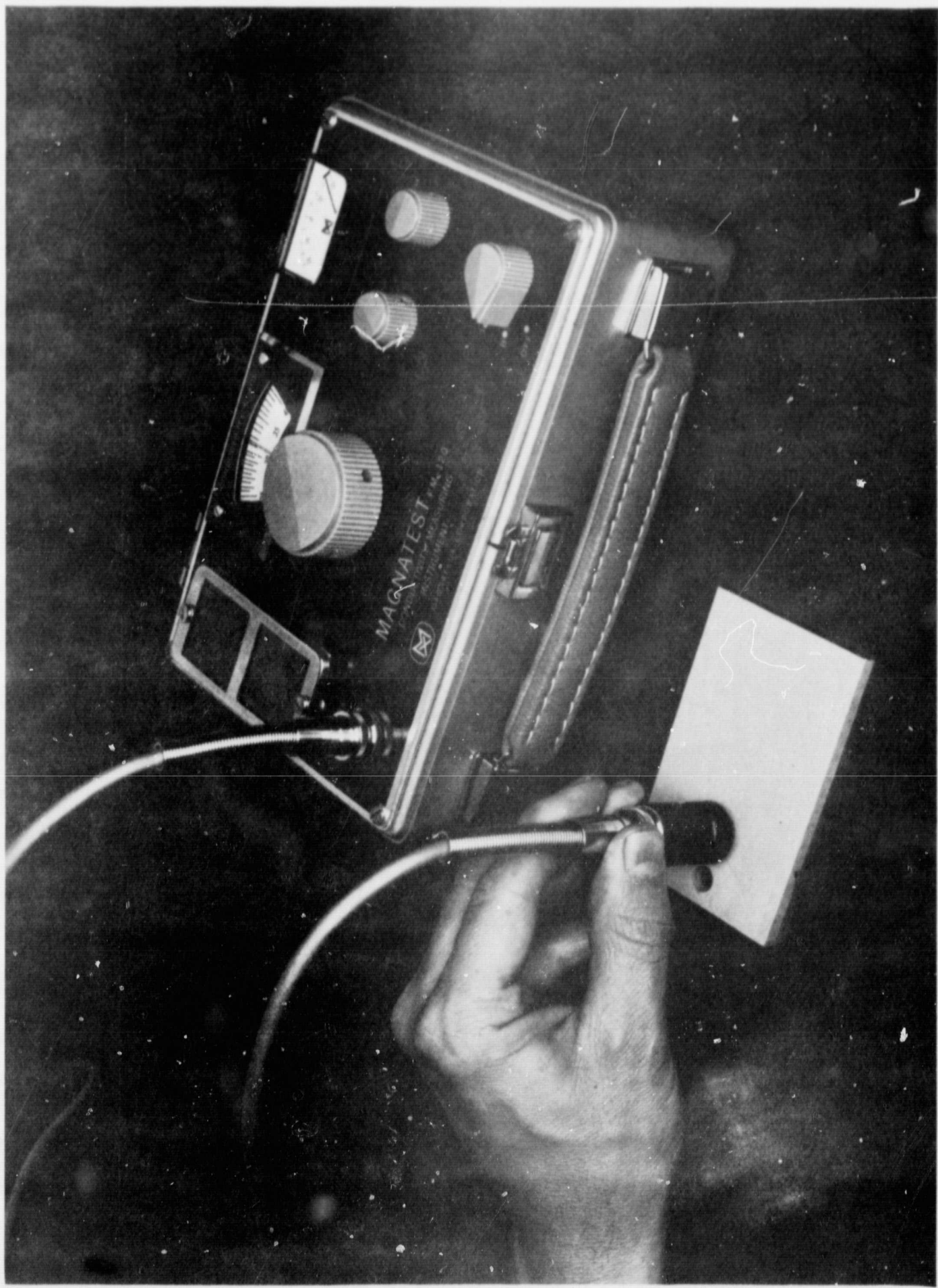
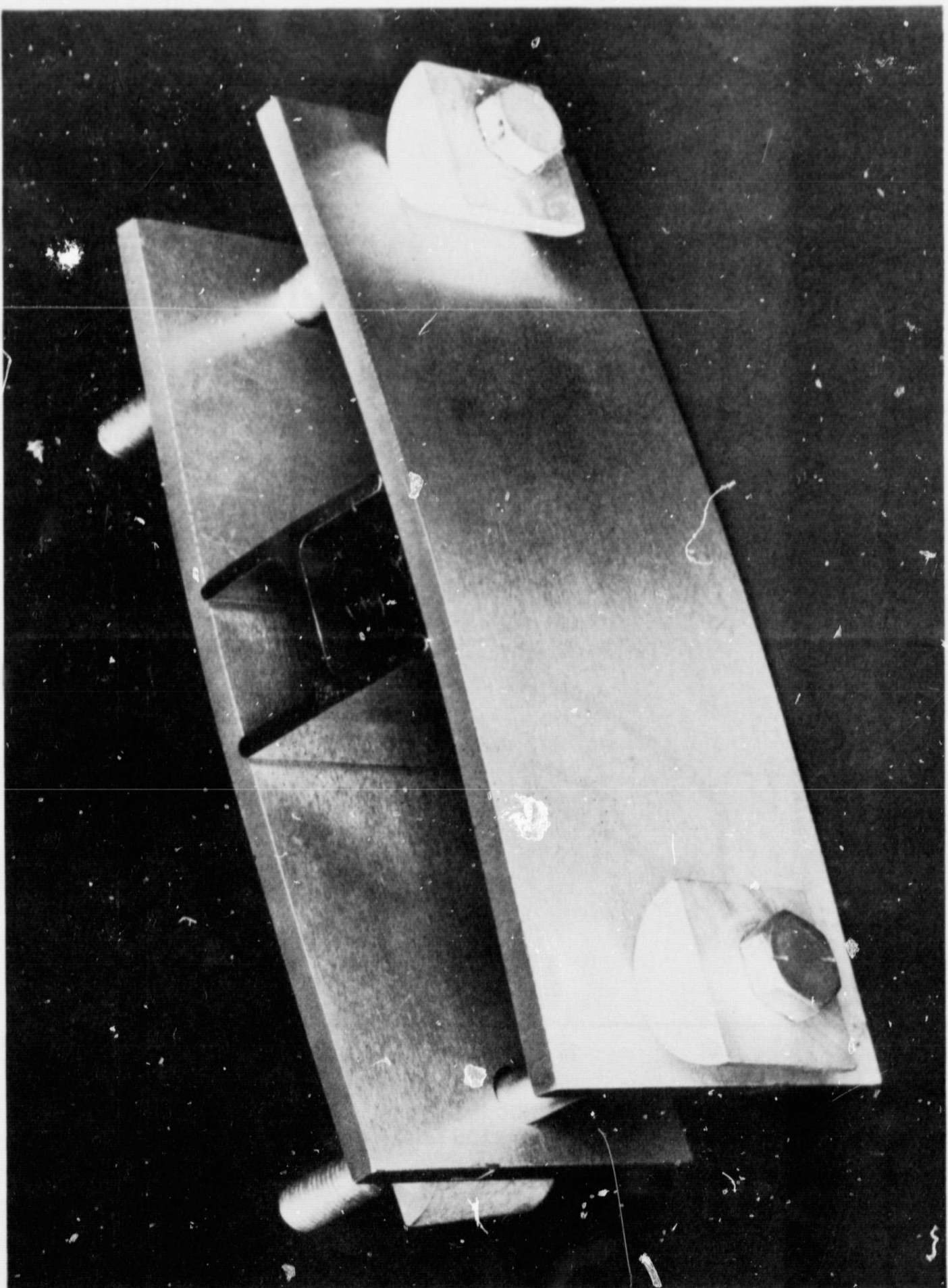
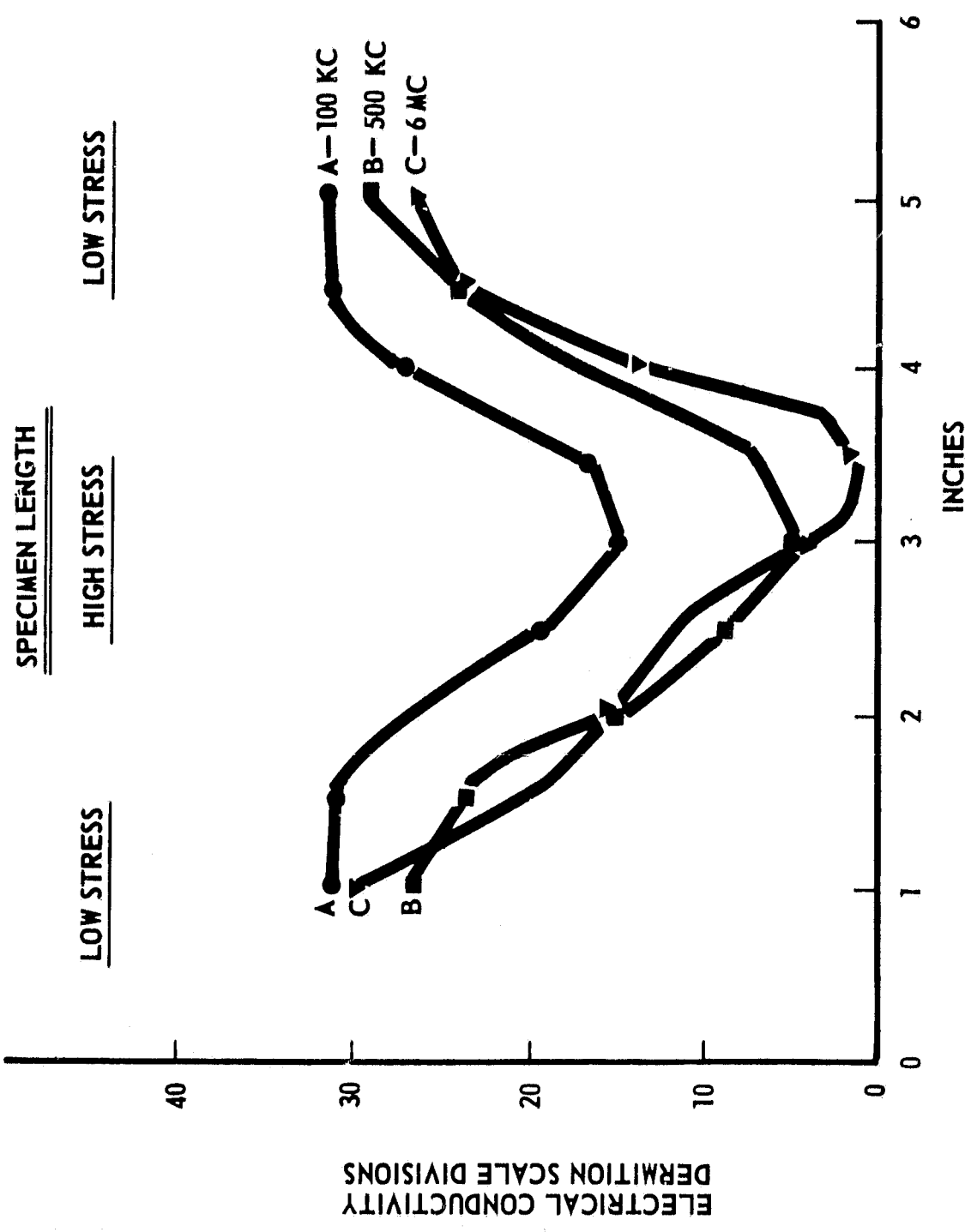


FIGURE 4: FLAT SPECIMEN STRESSING TECHNIQUE





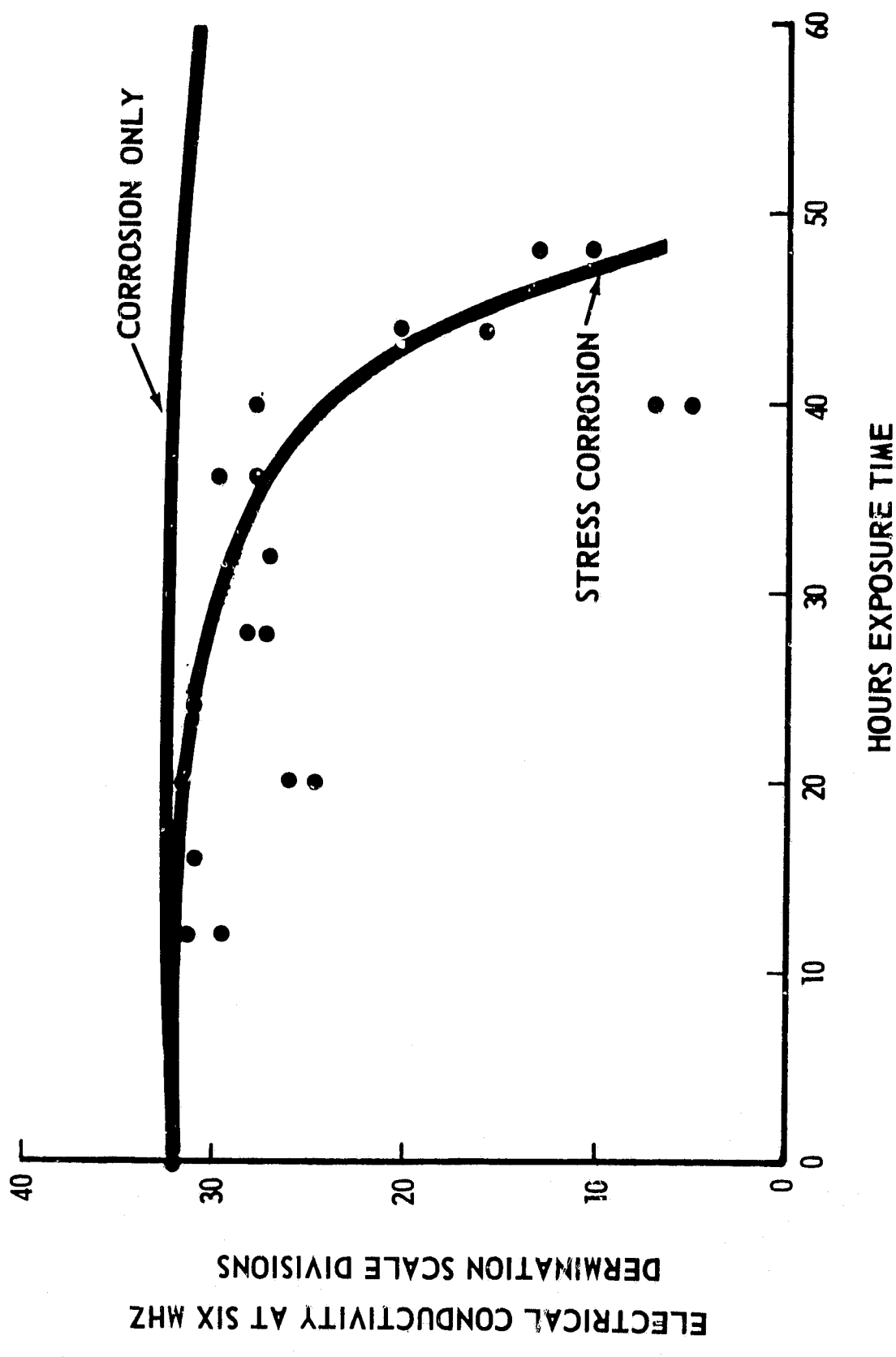


FIGURE 6: DEGRADATION OF 7079-T6 ALUMINUM BY STRESS CORROSION

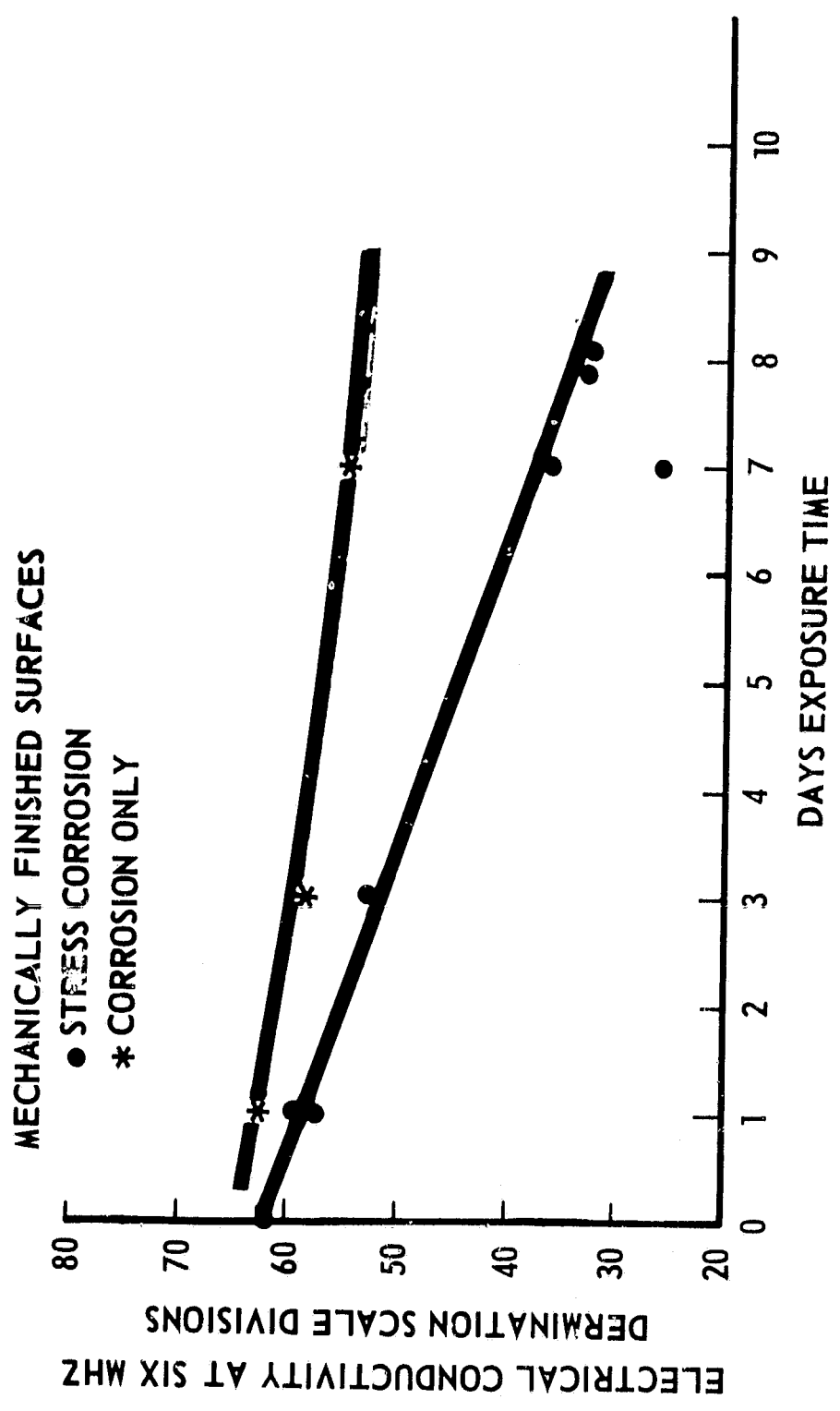


FIGURE 7: ELECTRICAL CONDUCTIVITY VS TIME
FOR CORRODED 2219-T31 ALUMINUM

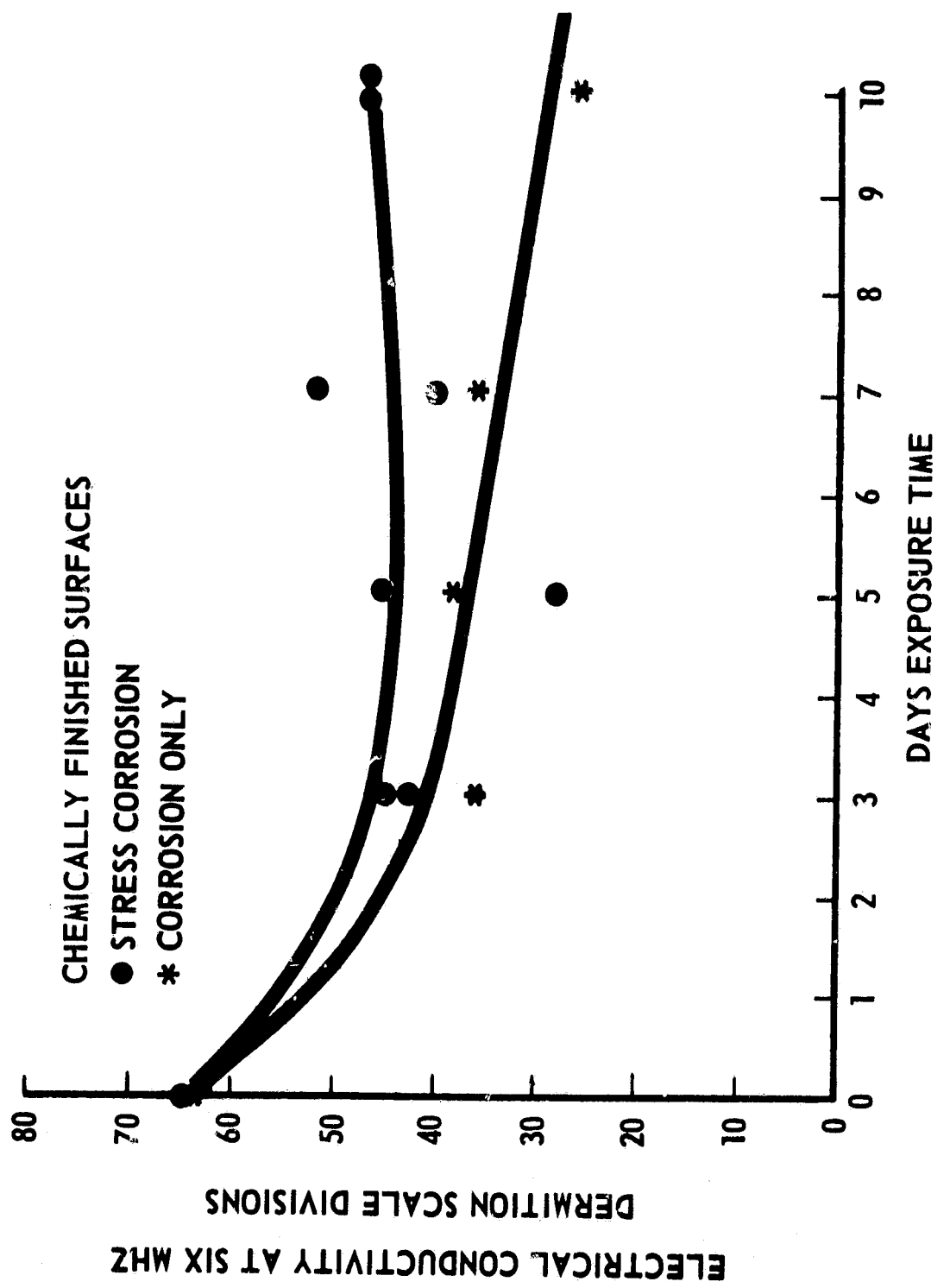


FIGURE 8: ELECTRICAL CONDUCTIVITY VS TIME FOR CORRODED 2219-T31 ALUMINUM

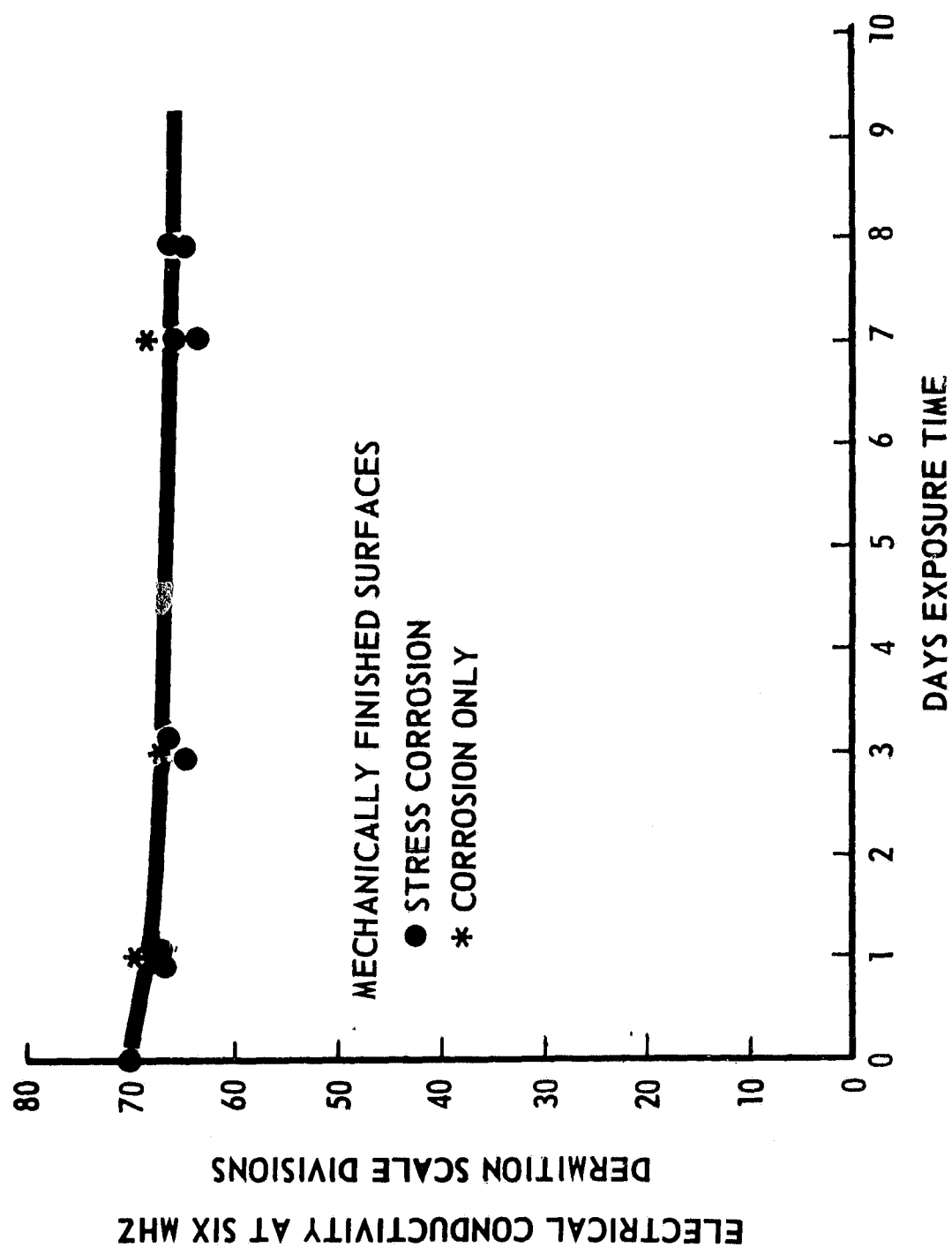
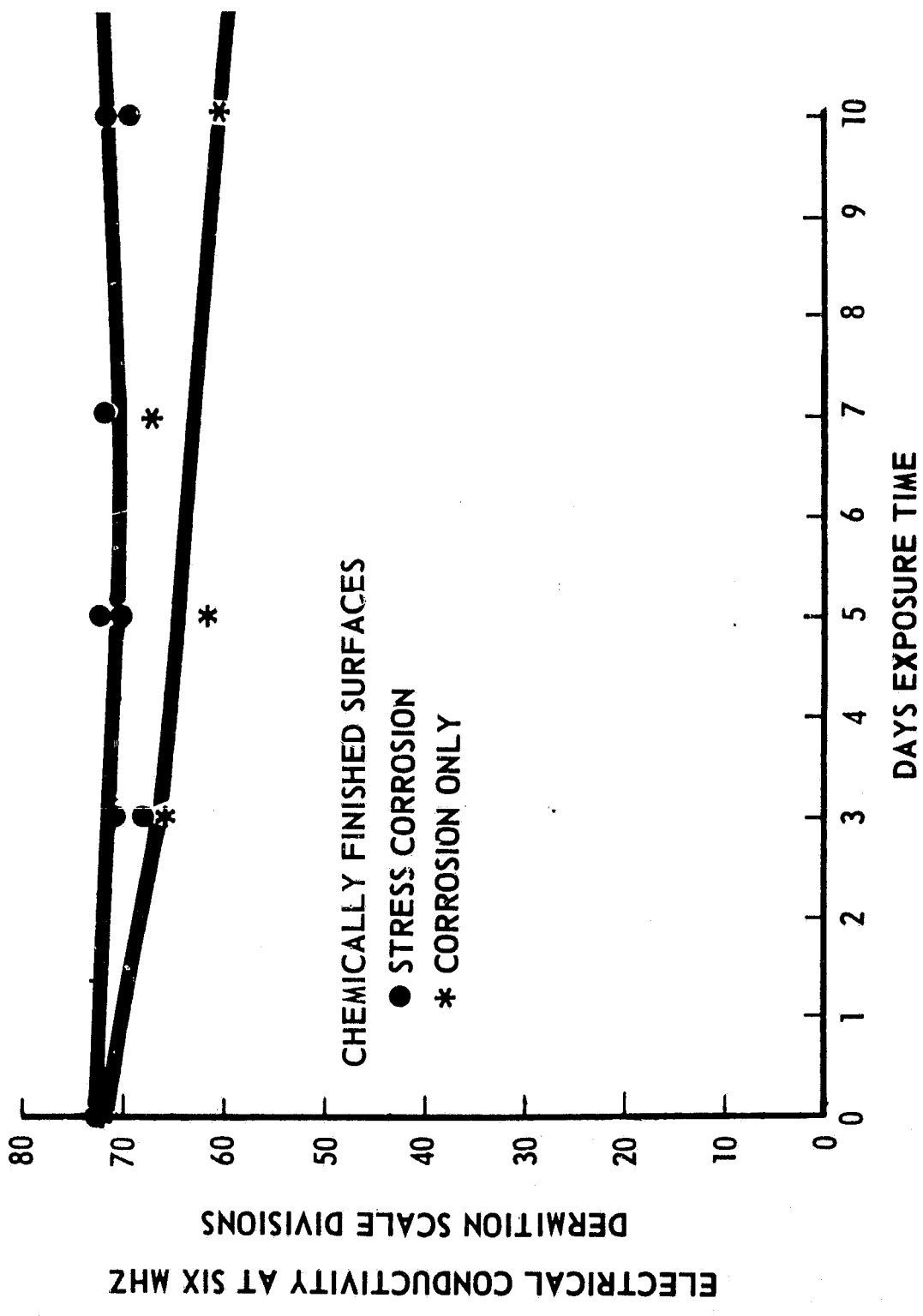
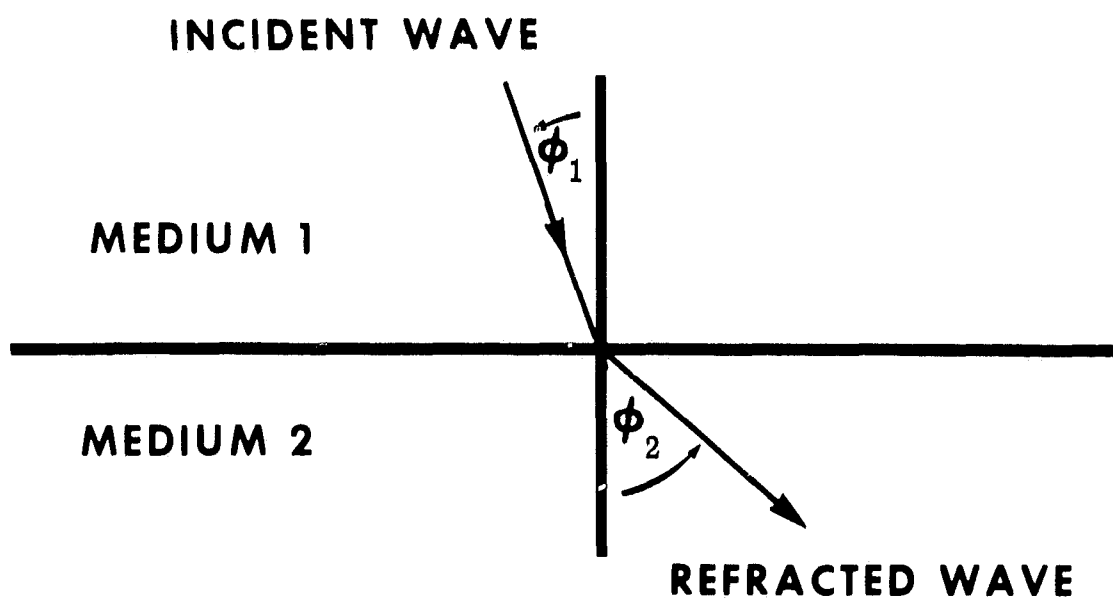


FIGURE 9: ELECTRICAL CONDUCTIVITY VS TIME FOR CORRODED 2219-T81 ALUMINUM



**FIGURE 10: ELECTRICAL CONDUCTIVITY VS TIME
FOR CORRODED 2219-T81 ALUMINUM**



$$\frac{\sin \phi_1}{\sin \phi_2} = \frac{V_1}{V_2}$$

WHERE V_1 = VELOCITY OF SOUND
IN FIRST MEDIUM

V_2 = VELOCITY OF SOUND
IN SECOND MEDIUM

FIGURE 11: SNELL'S LAW

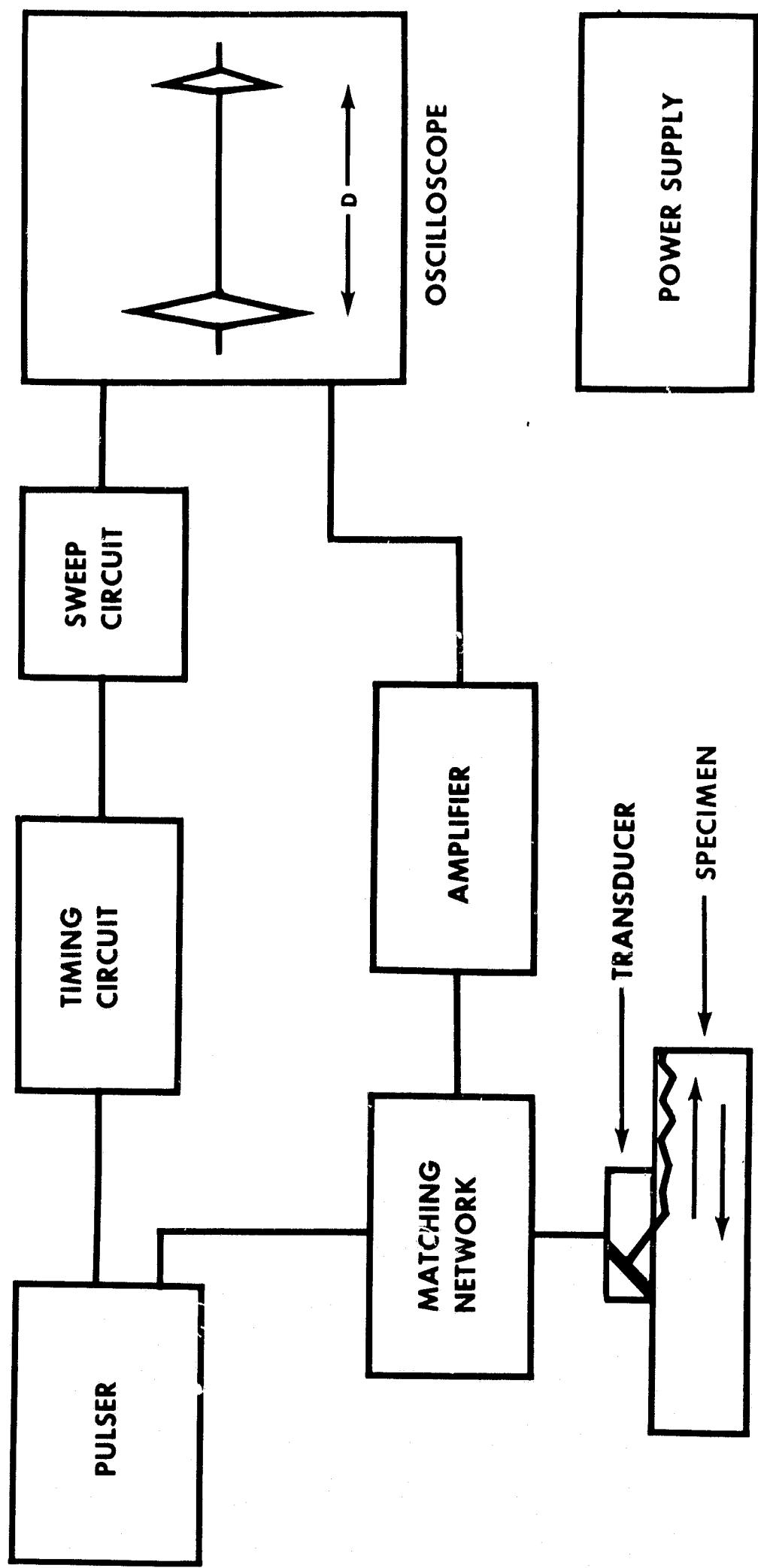


FIGURE 12: BLOCK DIAGRAM OF A TYPICAL ULTRASONIC SYSTEM

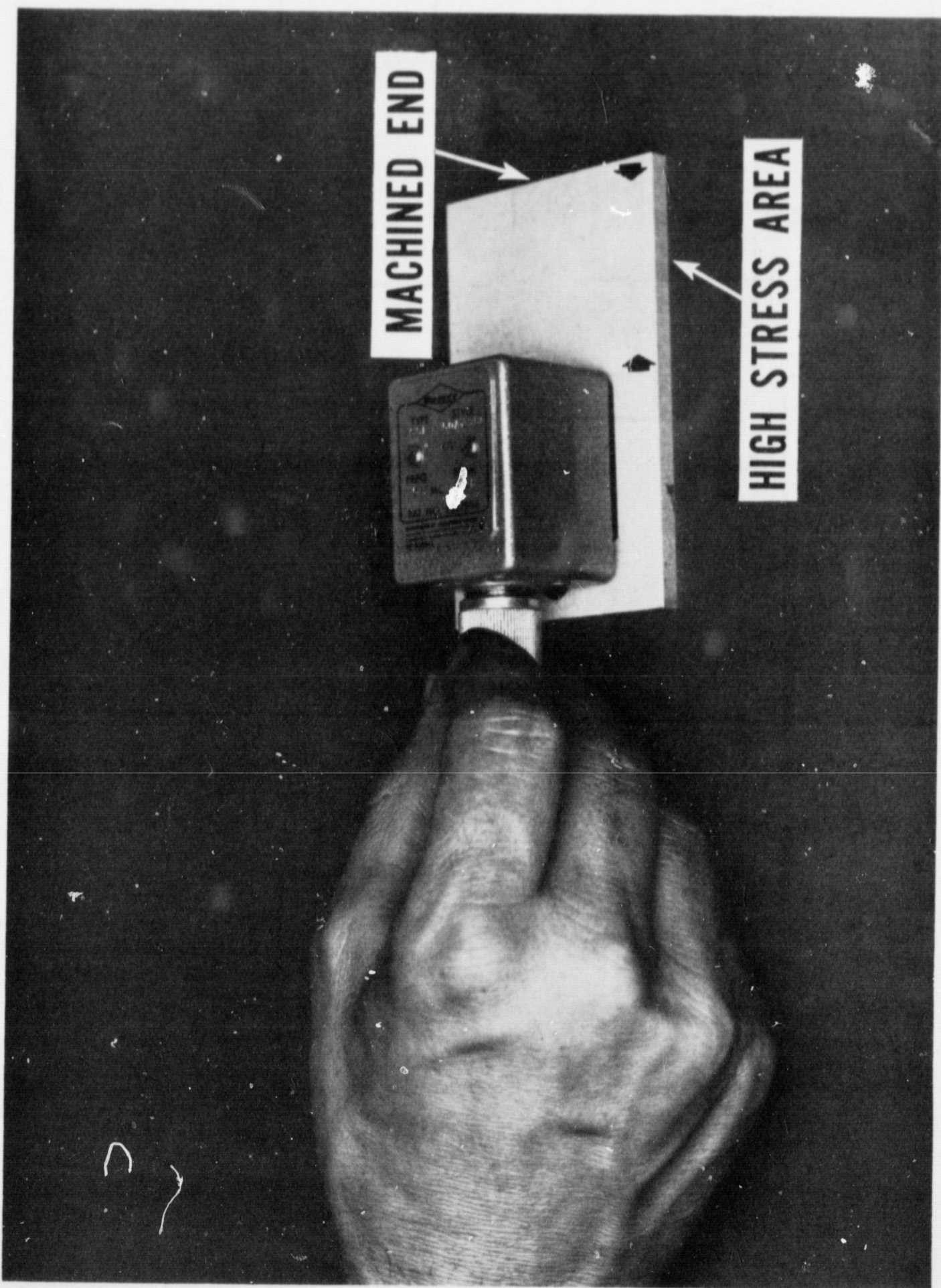
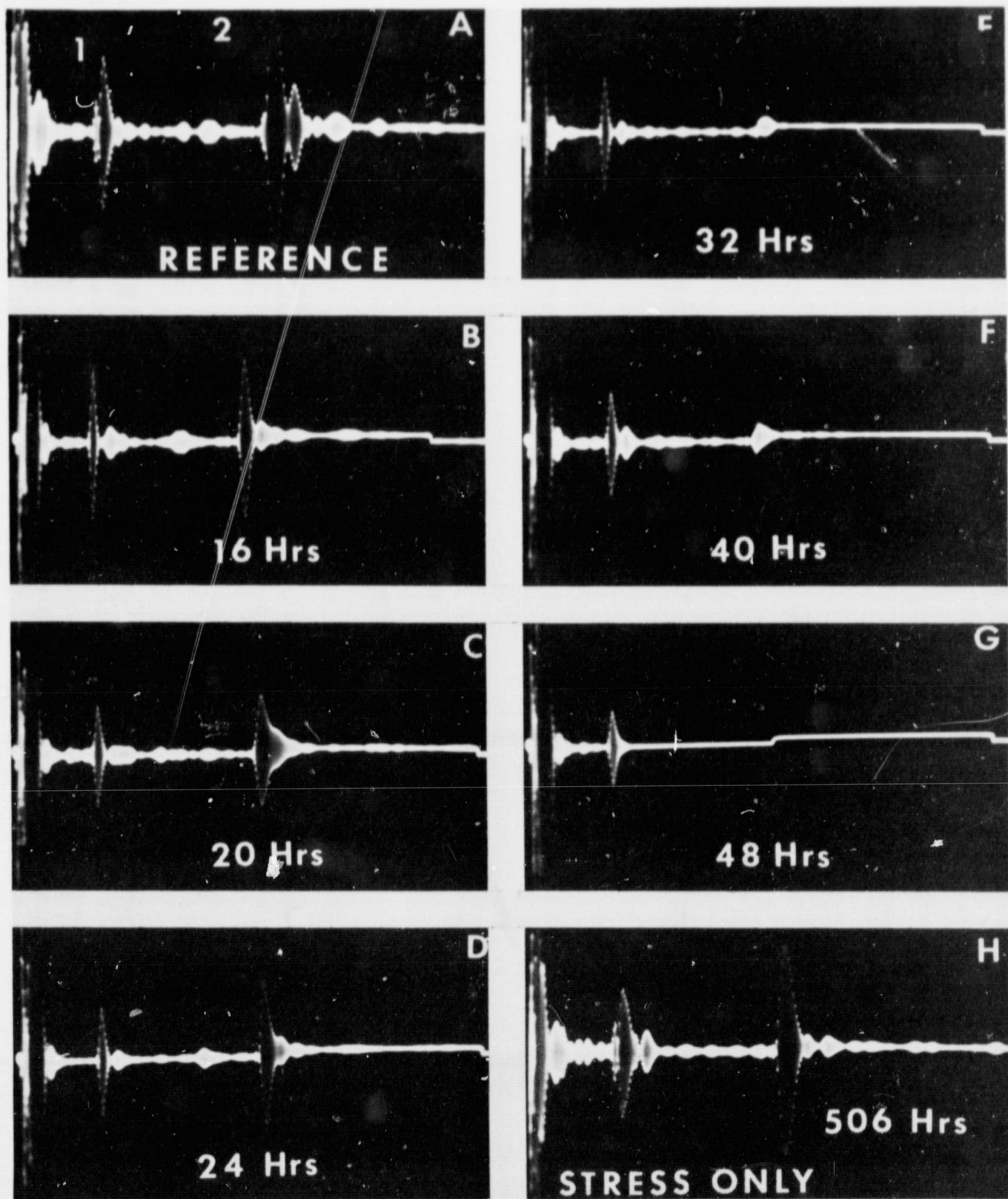


FIGURE 13: ULTRASONIC SURFACE WAVE TECHNIQUE



**FIGURE 14: ULTRASONIC SURFACE WAVE ATTENUATION
OF DEGRADED 7079-T6 ALUMINUM**

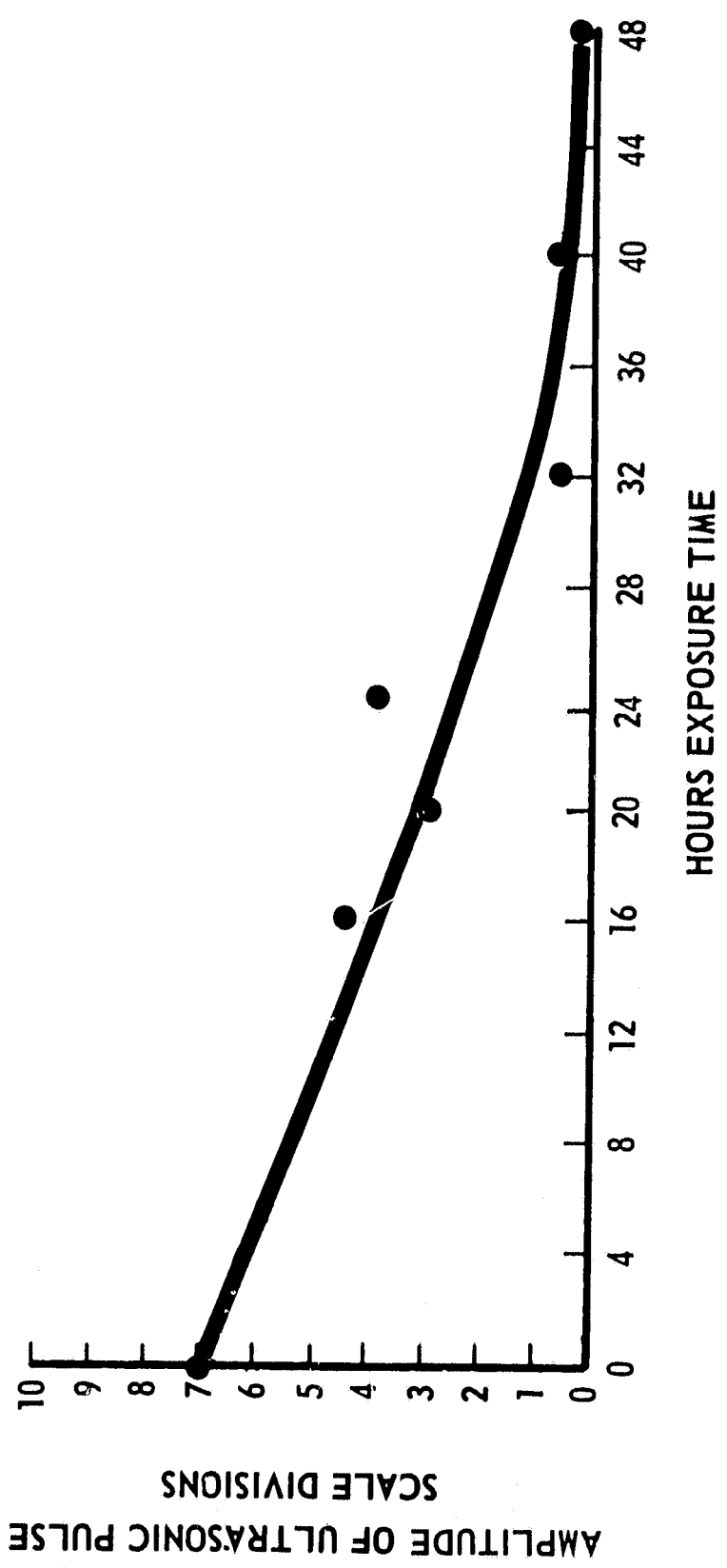


FIGURE 15: ATTENUATION OF 5 MHZ ULTRASONIC SURFACE WAVES IN CORRODED 7079-T6 ALUMINUM

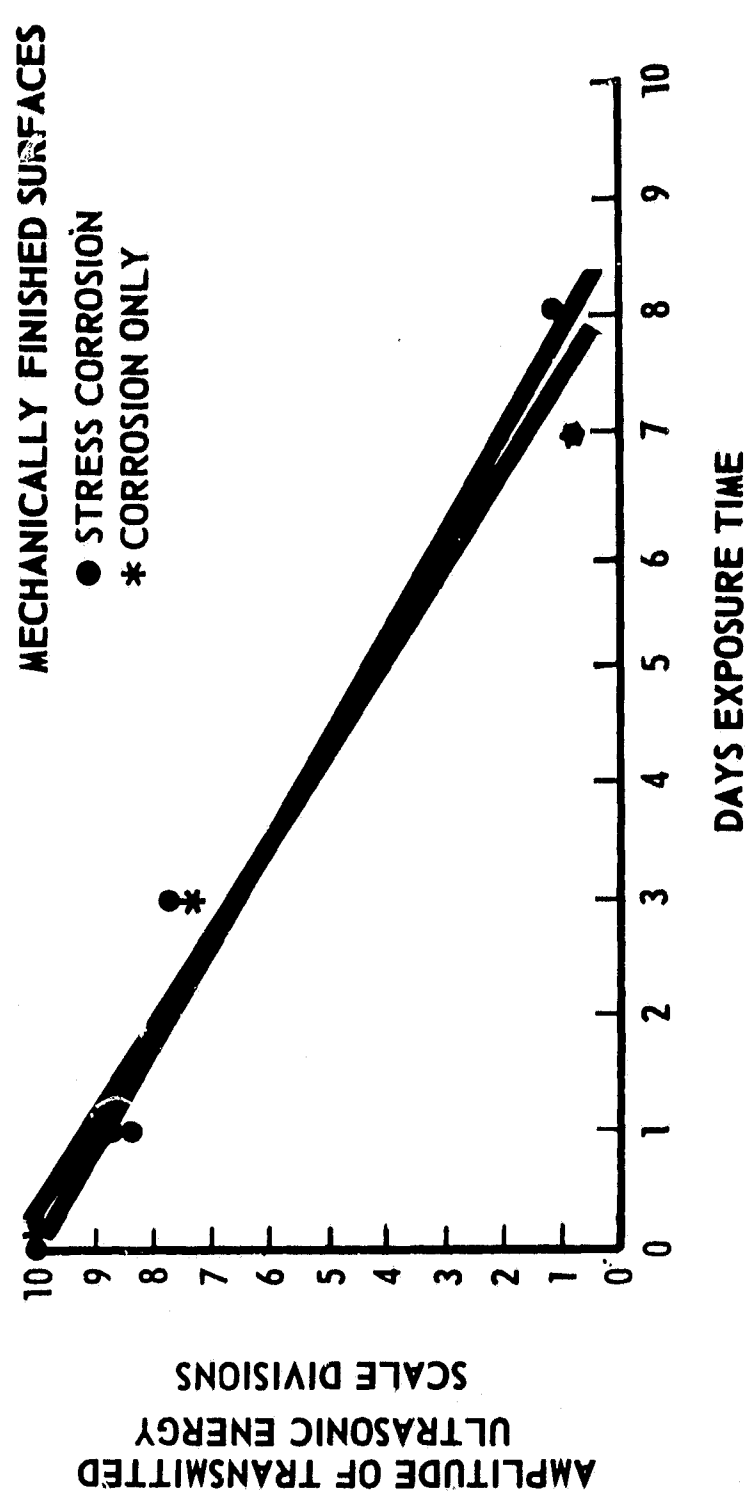


FIGURE 16: ATTENUATION OF 5 MHZ ULTRASONIC SURFACE WAVES IN CORRODED 2219-T31 ALUMINUM

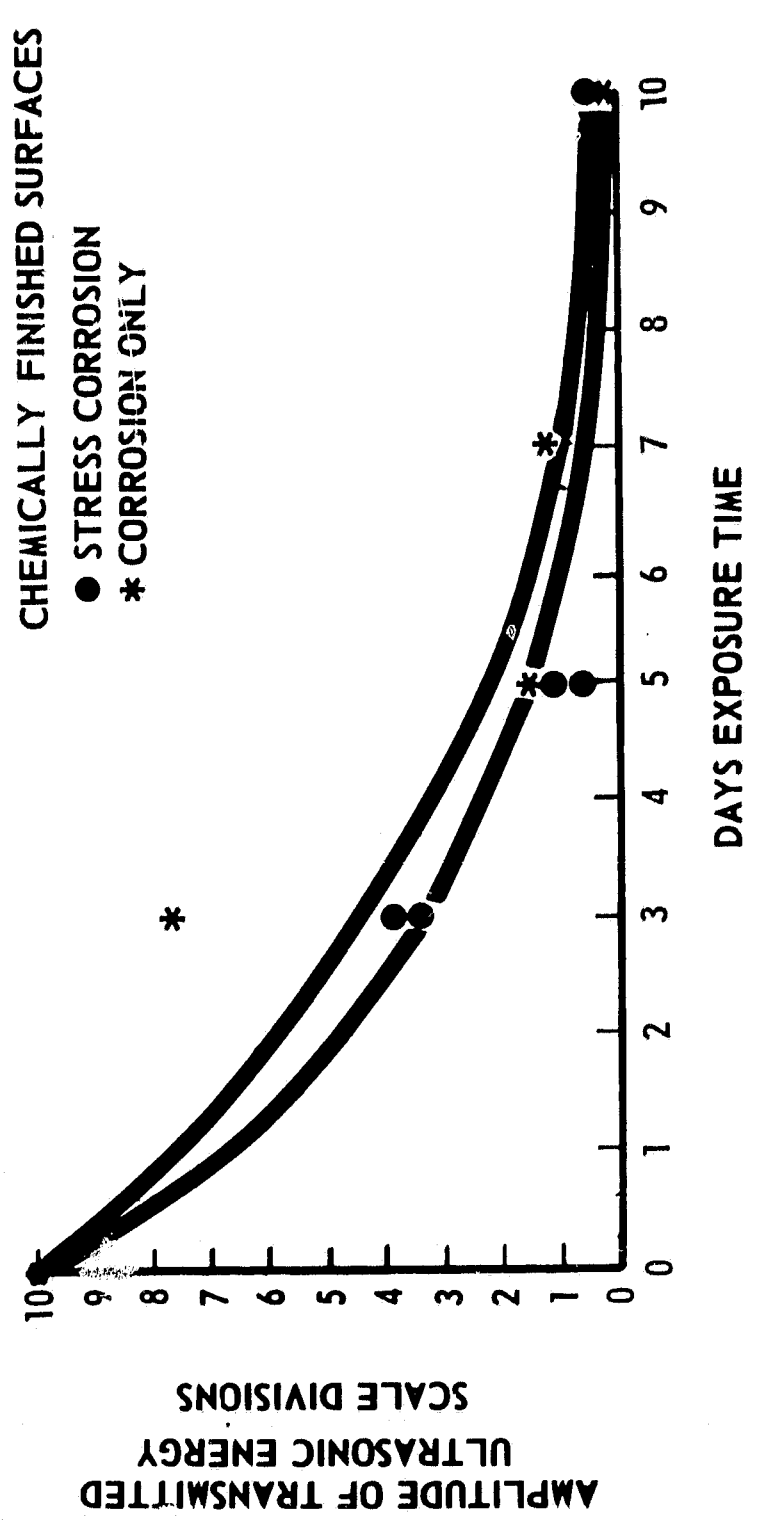


FIGURE 17: ATTENUATION OF 5 MHZ ULTRASONIC SURFACE WAVES IN CORRODED 2219-T31 ALUMINUM

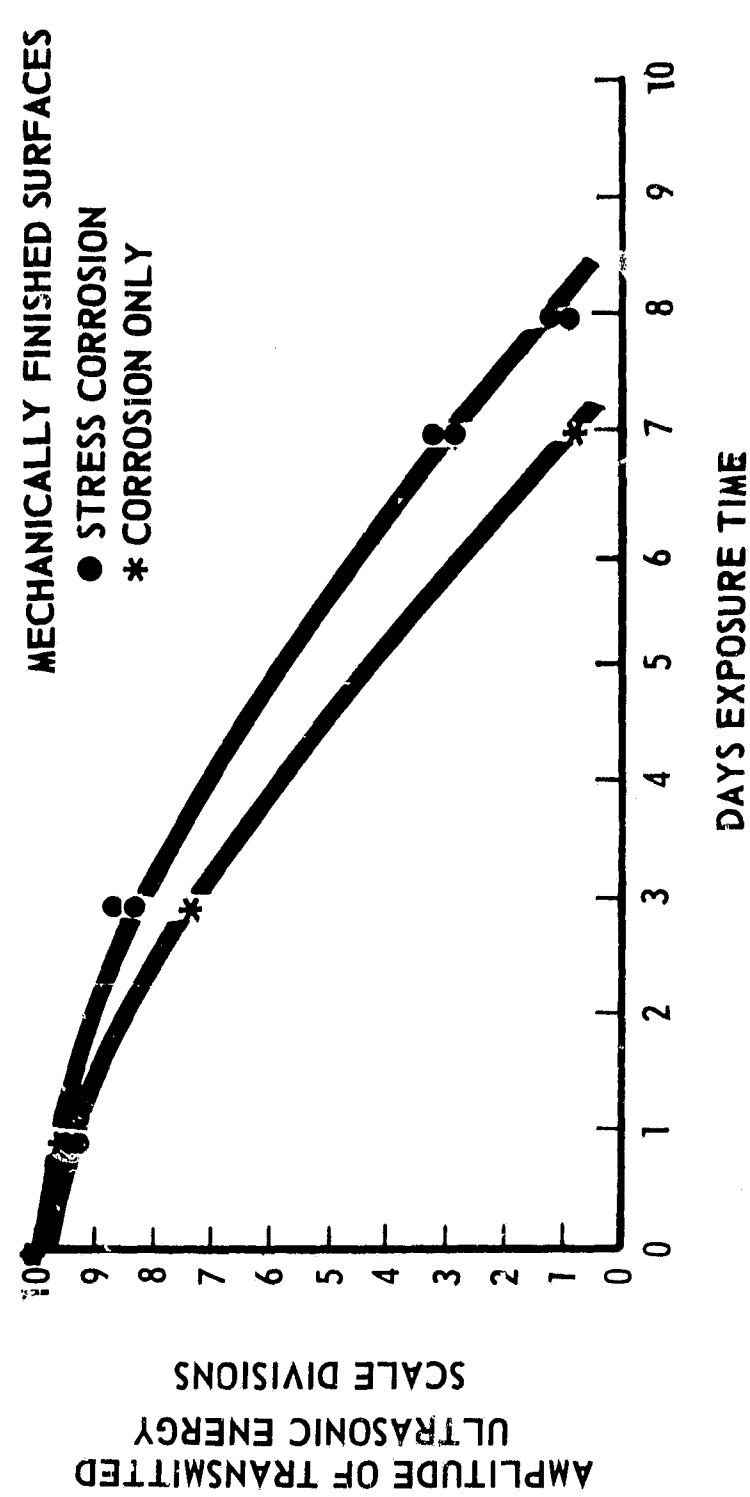


FIGURE 18: ATTENUATION OF 5 MHZ ULTRASONIC SURFACE WAVES IN CORRODED 2219-T81 ALUMINUM

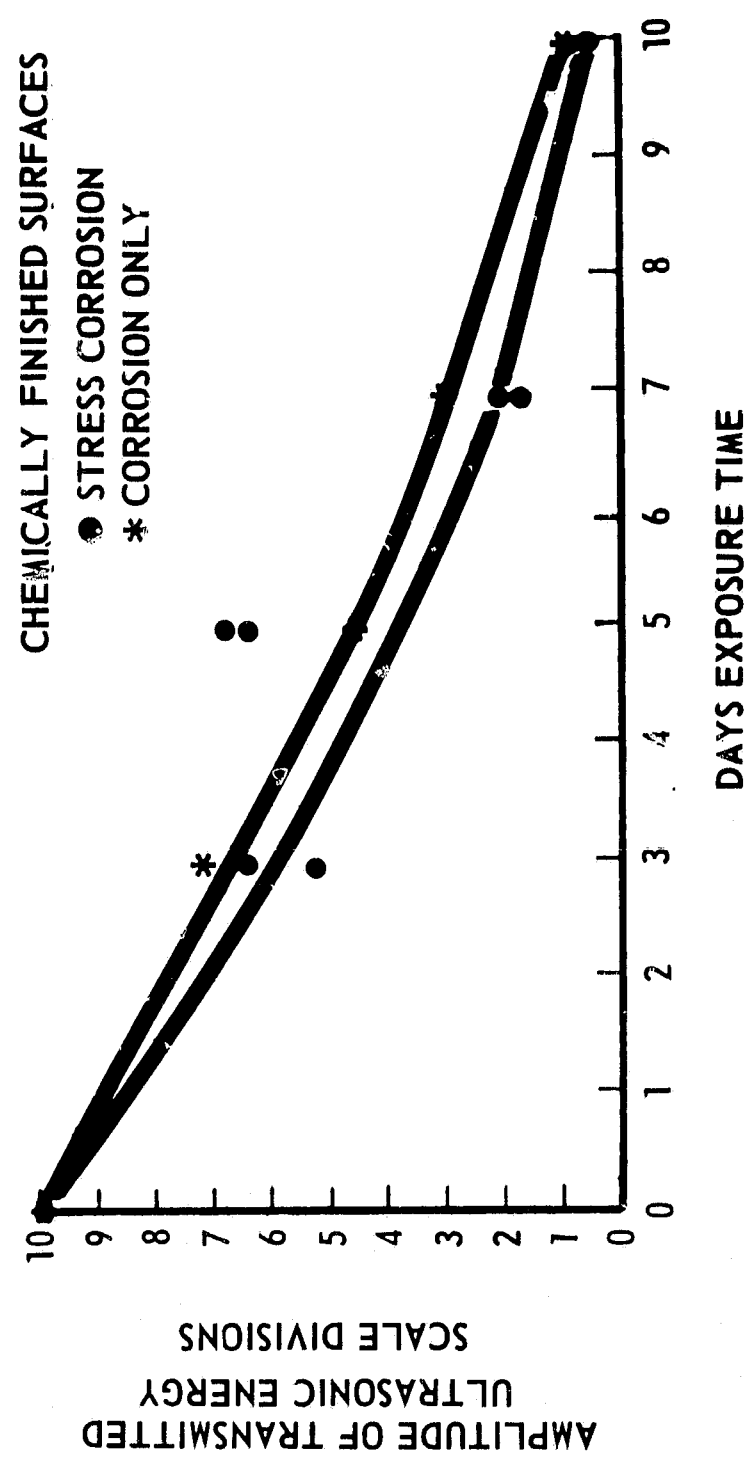


FIGURE 19: ATTENUATION OF 5 MHZ ULTRASONIC SURFACE WAVES IN CORRODED 2219-T81 ALUMINUM

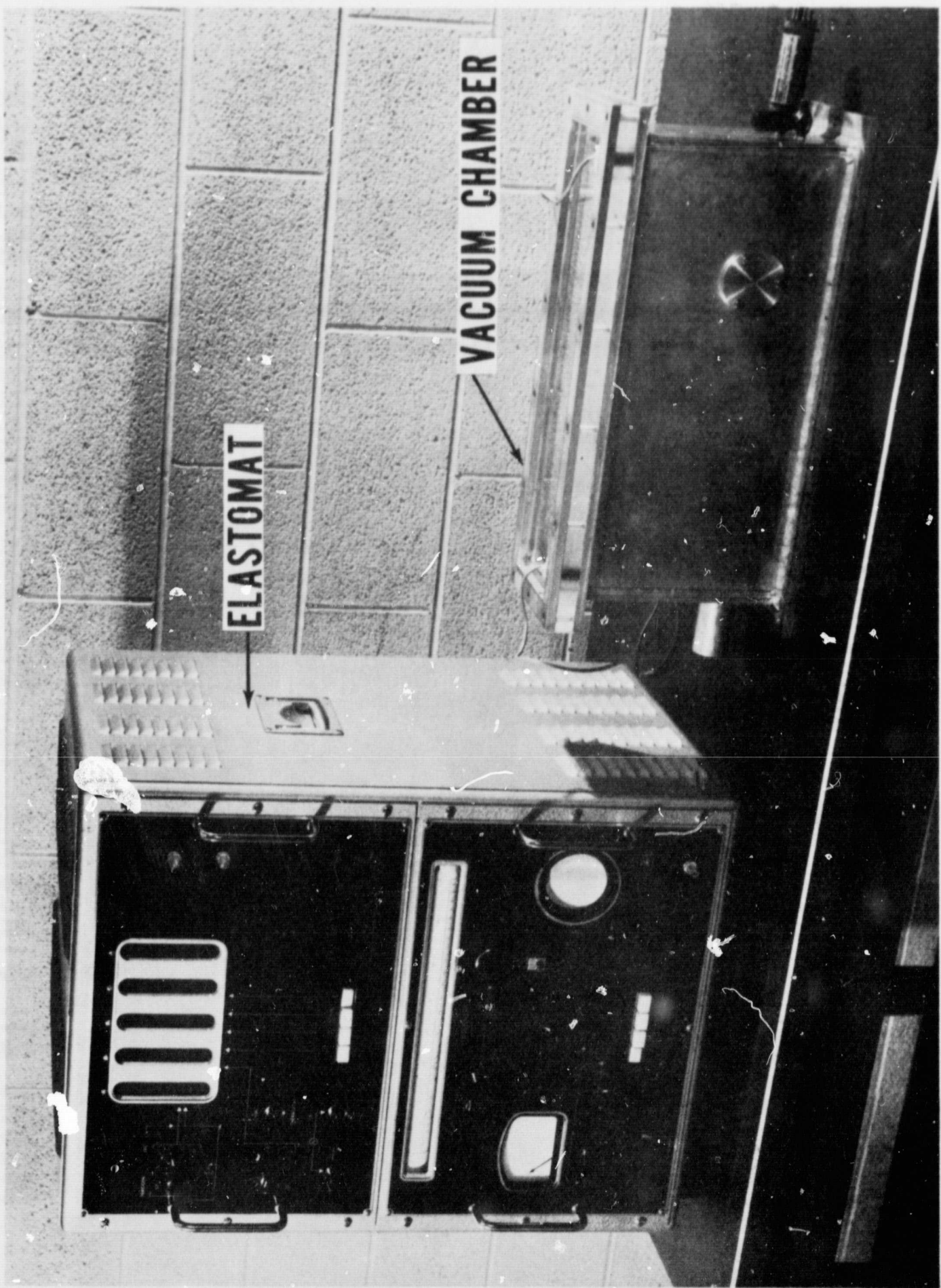


FIGURE 20: ELASTOMAT AND VACUUM CHAMBER

FIGURE 21: STRESSING FIXTURE FOR CYLINDRICAL SPECIMEN

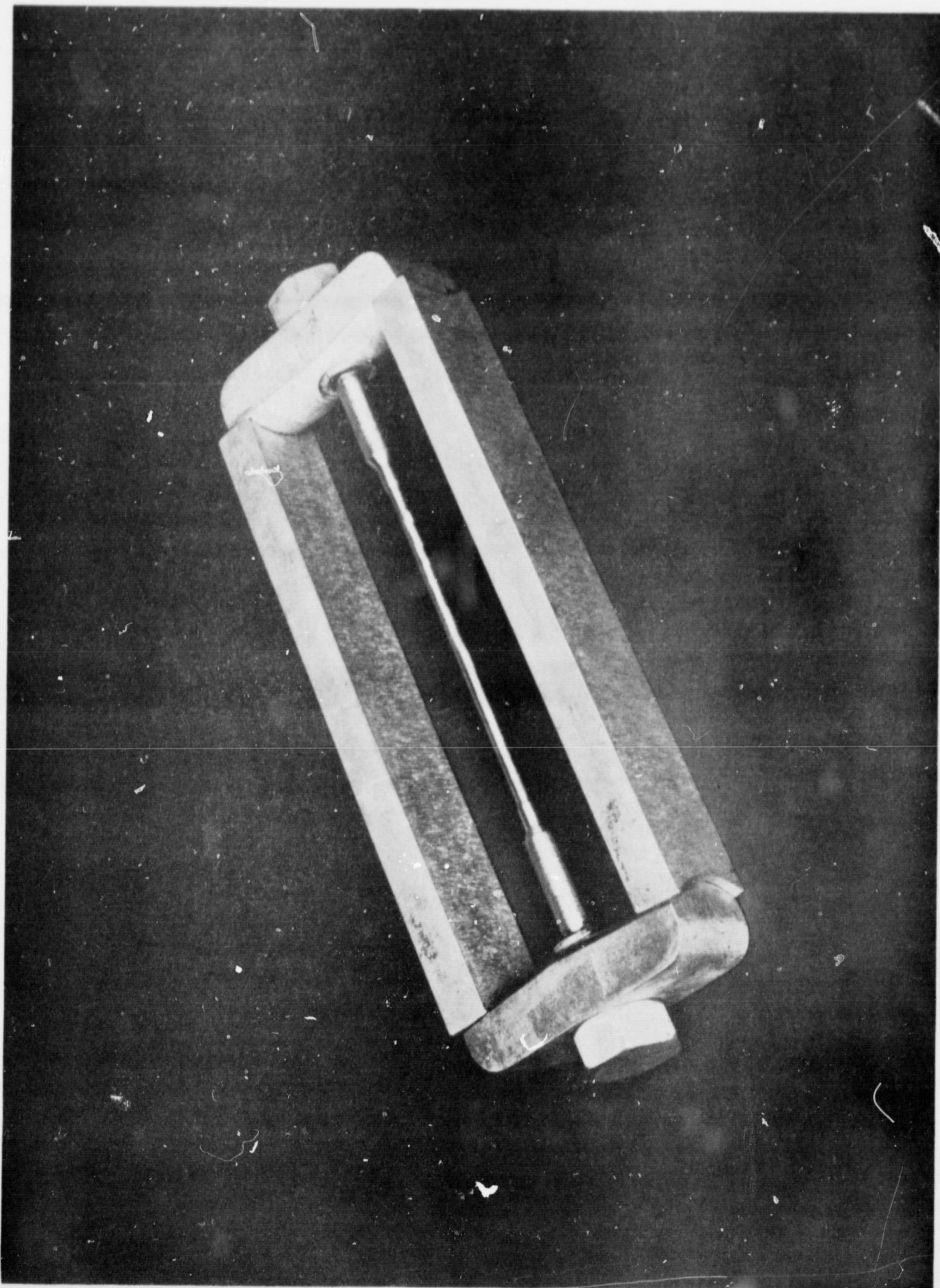
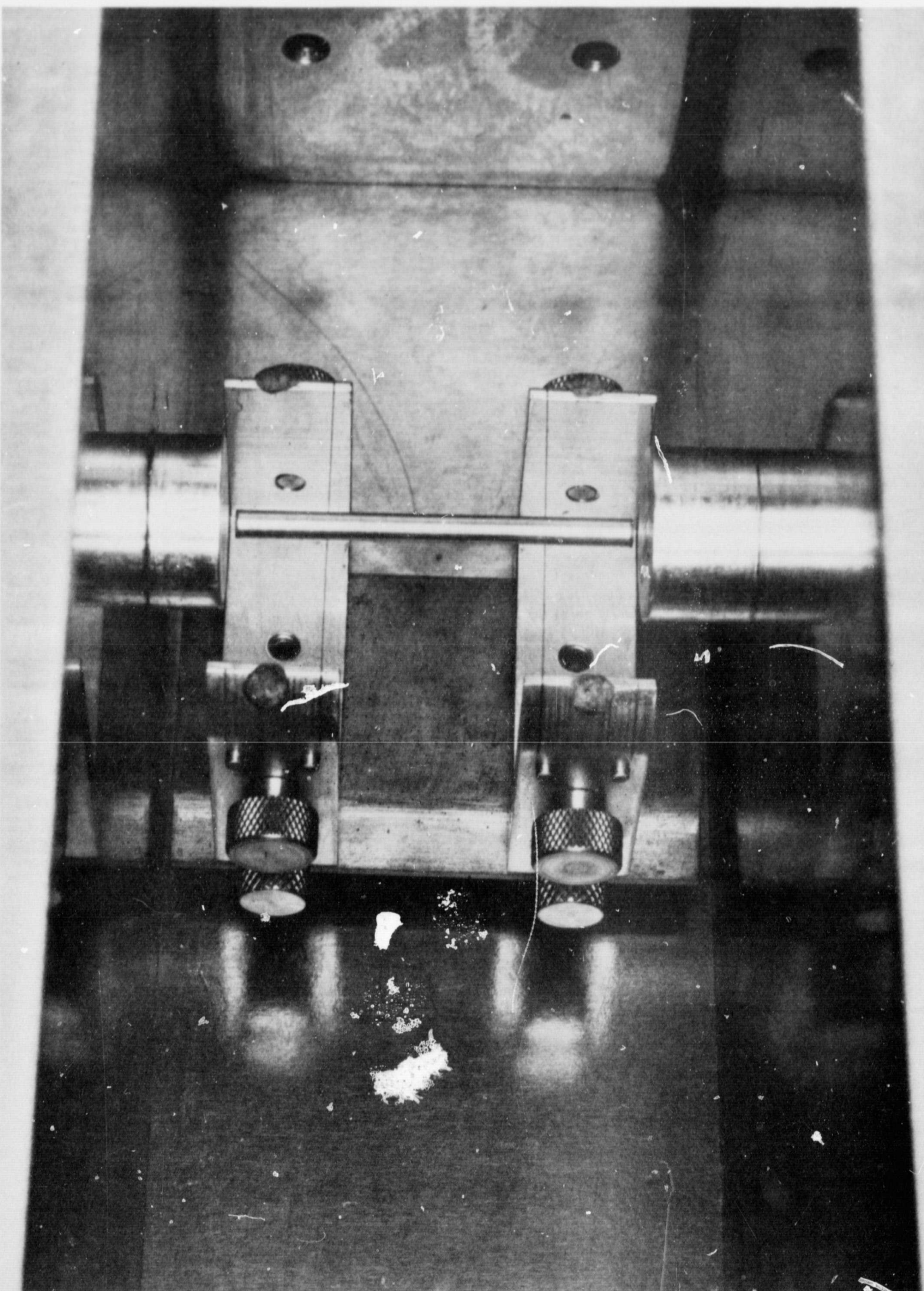


FIGURE 22: SPECIMEN SUPPORT FOR INTERNAL FRICTION MEASUREMENTS



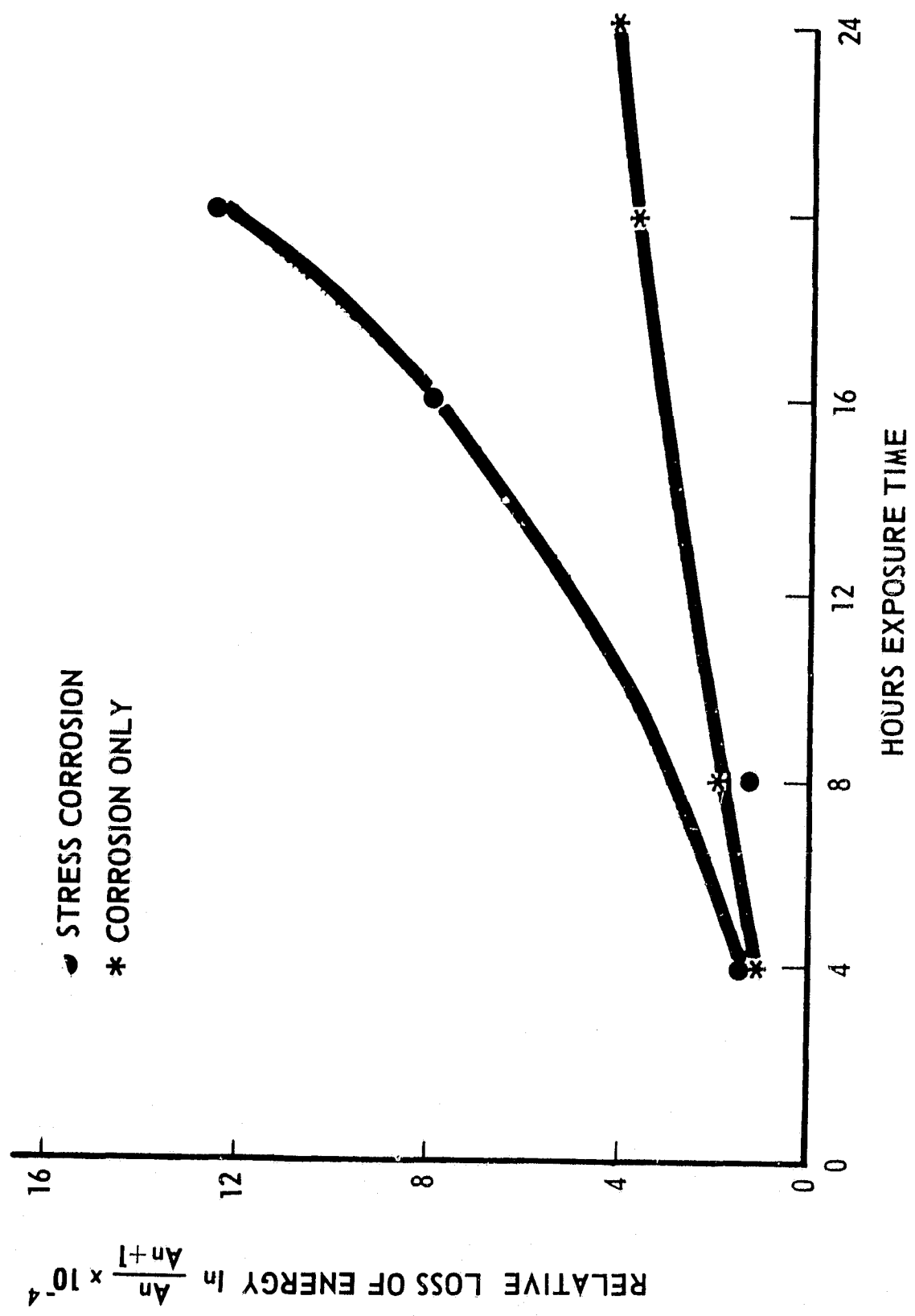


FIGURE 23: INTERNAL FRICTION OF 7079-T6 ALUMINUM VIBRATING IN THE TRANSVERSE MODE

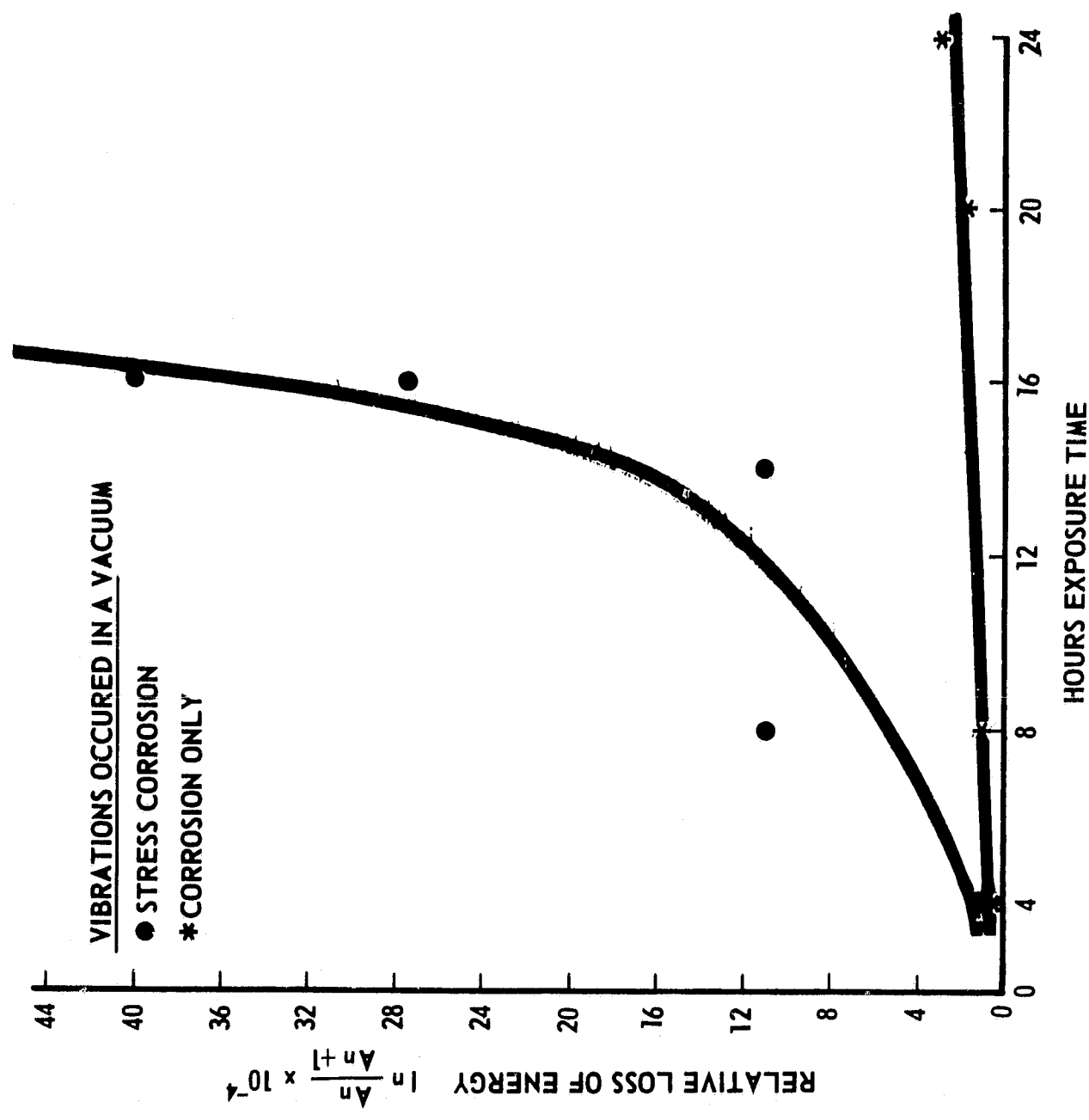


FIGURE 24: INTERNAL FRICTION OF CORRODED 7079-T6 ALUMINUM VIBRATING IN THE TORSIONAL MODE

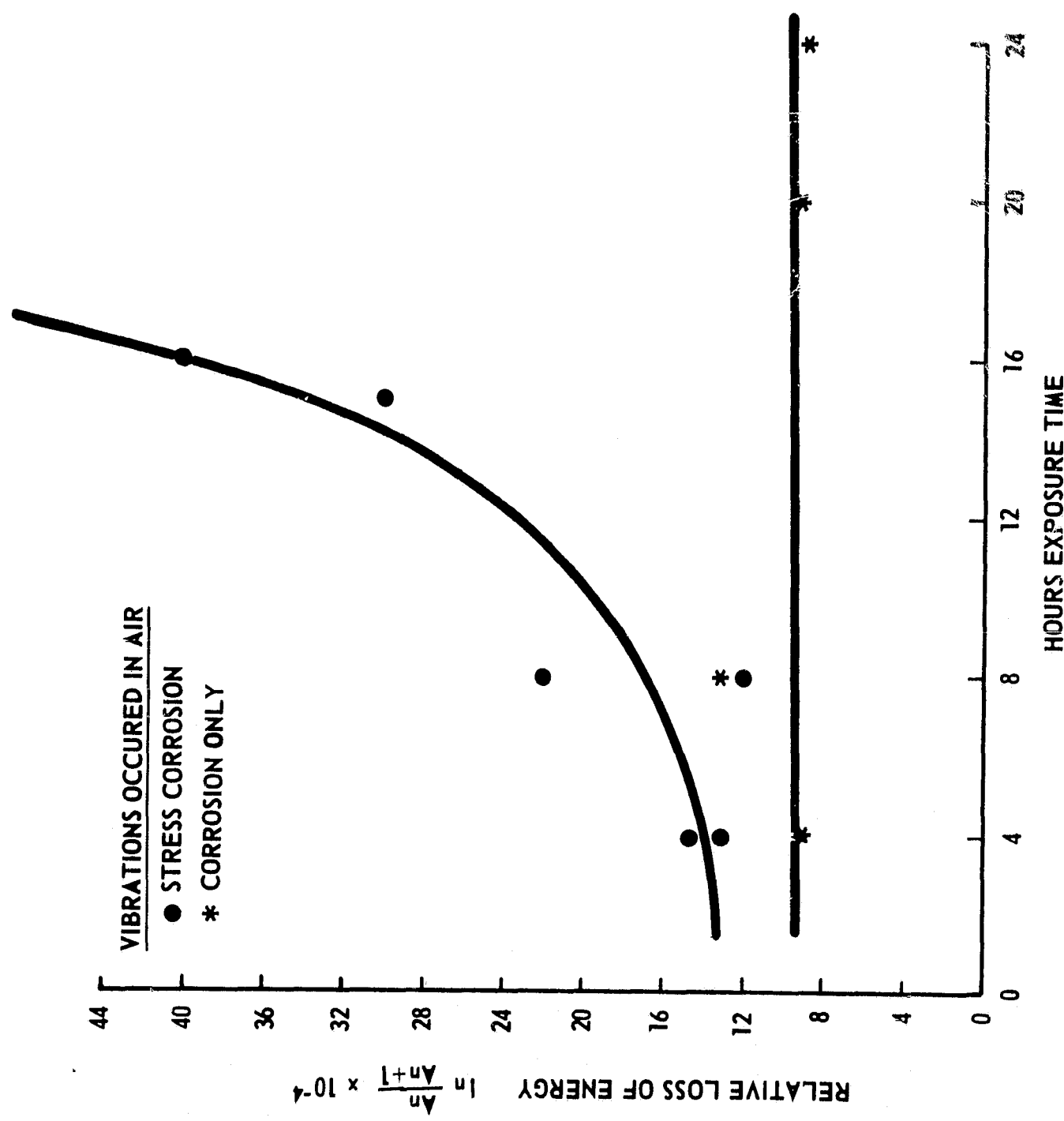


FIGURE 23: INTERNAL FRICTION OF CORRODED 7079-T6 ALUMINUM VIBRATING IN THE TORSIONAL MODE

REFERENCES

1. Personnel of Battelle Memorial Institute: Stress Corrosion Cracking of Aluminum Alloys, DMIC Memorandum 202.
2. Chalmers, Bruce and Quarrell, A. G.: The Physical Examination of Metals, Arnold, 1960.
3. Engineers of Westinghouse: Westinghouse Industrial Electronics Reference Book, Wiley, 1948.
4. Truell, R.: Basic Research in Ultrasonics, Watertown Arsenal, 1959.
5. Carlin, Benson: Ultrasonics, McGraw-Hill, 1960.
6. Stanford, E. G. and Pearson, J. H.: Progress in Nondestructive Testing, Volume 1. Heywood, 1958.
7. Mason, Warren P.: Physical Acoustics and the Properties of Solids, D. Van Nostrand, 1958.
8. Bordoni, P. G.: Relaxation of Lattice Imperfections in Solids, Proceedings of the International School of Physics. Academic Press, 1963.

August 23, 1968

APPROVAL

NASA TM X-53772

THE NONDESTRUCTIVE EVALUATION OF STRESS CORROSION
INDUCED PROPERTY CHANGES IN ALUMINUM

by

W. N. Clotfelter, B. F. Bankston, and E. E. Zachary

The information in this report has been reviewed for security classification. Review of any information concerning Department of Defense or Atomic Energy Commission programs has been made by the MSFC Security Classification Officer. This report, in its entirety, has been determined to be unclassified.

This document has also been reviewed and approved for technical accuracy.

E. C. McKannan

E. C. McKannan
Chief, Engineering Physics Branch

J. E. Kingsbury

J. E. Kingsbury
Chief, Materials Division

W. R. Lucas

W. R. Lucas
Director, Propulsion and Vehicle Engineering Laboratory